

# IMPROVE DATA USER GUIDE 2023 (VERSION 2)

J.L. Hand (24 October 2023)

Version 1.0 1995 User Guide can be found [here](#).

## TABLE OF CONTENTS

1. Introduction.....	1
2. Routine Monitoring.....	1
3. Aerosol Sampling and Analysis.....	3
4. Accessing and Downloading IMPROVE Data from FED website .....	5
5. Data Processing.....	7
6. Data Validation .....	9
7. Calculated Mass Variables (IMPROVE Report VI).....	10
8. Reconstructed Light Extinction Coefficients.....	13
9. Data Usage.....	15
10. Trends .....	16
11. References.....	18
Appendix A. Site locations.....	22
Appendix B. Tables from the Federal Land Manager Environmental Database .....	28
Appendix C. Status Flags and Codes .....	34
Appendix D. Uncertainty Estimates .....	36

## 1.0 INTRODUCTION

The IMPROVE Data User Guide provides information for the general user on routine monitoring, aerosol sampling and analysis, accessing and downloading data, descriptions of methods for determining concentrations, minimum detection limits, uncertainties, calculated variables, mass and aerosol extinction reconstruction algorithms, and other applicable information for obtaining, analyzing and interpreting IMPROVE data. The guide will periodically be updated as new information is available or changes occur.

Information in this Guide is reproduced or summarized from several documents that provide additional details regarding the operation of the IMPROVE network and reporting of IMPROVE data. These documents are available [online](#) and include:

- IMPROVE [Standard Operating Procedures \(SOP\)](#)
- IMPROVE [Quality Assurance and Control Reports](#)
- IMPROVE [Data Advisories](#)
- IMPROVE [Reports](#)

## 2.0 ROUTINE MONITORING

The IMPROVE program began operating in 1987, with network monitoring initiated in March of 1988 at nearly 40 sites in Class I areas (CIAs). The network expanded and grew to

about 70 sites through the 1990s. The monitoring sites were mostly in remote areas and all used the same instrumentation, monitoring, and analysis protocols. Adjustments to the suite of measurements occurred on several occasions due to scientific considerations or resource and funding limitations. Several of the sites also included optical monitoring with a nephelometer or a transmissometer and scene monitoring with color photography to document scenic appearance (Malm et al., 1994, Hand et al., 2023).

With the promulgation of the [Regional Haze Rule](#) (RHR) in 1999, the IMPROVE network expanded, with 110 sites chosen to represent regional haze in 155 of the 156 CIAs, the Bering Sea Wilderness being the exception. Details regarding the selection process of additional sites is provided in [IMPROVE Report III](#) (Malm et al., 2000). The 110 sites are referred to as IMPROVE sites, while other sites, sponsored by federal, state and other organizations, are referred to as IMPROVE protocol sites. All sites use the same instrumentation, monitoring, and analysis protocols. In 2023, the network consisted of 227 sites (157 operating and 70 discontinued). The sites are often grouped by region, an empirical categorization that regionally organizes sites based on similar aerosol species concentrations and seasonal patterns. There are 36 IMPROVE regions: 29 rural, four urban (including both long-term urban sites and urban quality assurance sites), and three international sites. Some rural regions may have only one site (e.g., Death Valley, Lone Peak, Virgin Islands). A map of the site locations is shown in Figure 1 and a list of site locations is provided in Appendix A, which includes the site name, site code, state, latitude, longitude, elevation, and dates of operation. Similar information is available as [tables](#) on the IMPROVE website and in the [IMPROVE Report VI](#) (Hand et al., 2023).

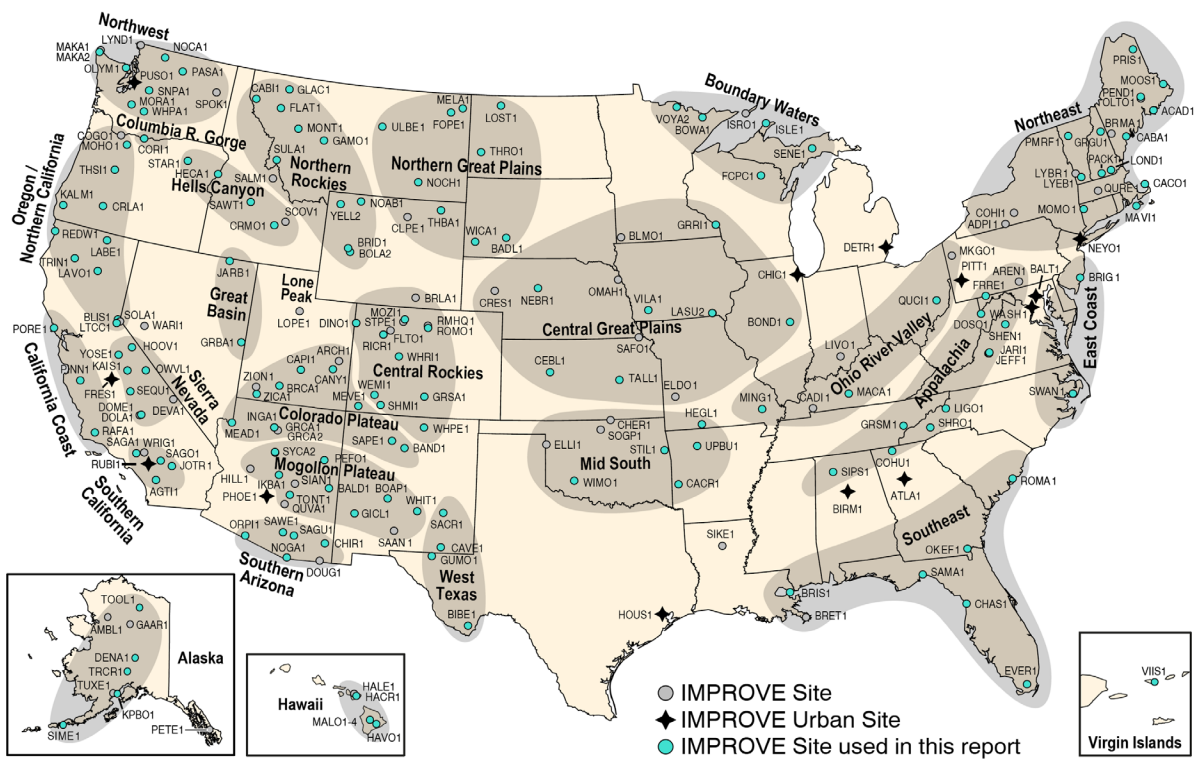


**Figure 1. Locations of IMPROVE sites for all discontinued and current sites. IMPROVE regions are indicated by shading and bold text. Urban IMPROVE sites are identified by stars. Cyan circles indicate sites with data used in the analyses in the [IMPROVE VI report](#) (Hand et al., 2023).**

### 3.0 AEROSOL SAMPLING AND ANALYSIS

IMPROVE filters are collected routinely every third day from midnight to midnight local standard time and data are reported at local conditions throughout the network. The IMPROVE sampler consists of four independent modules (A, B, C, and D; see Figure 2). Each module incorporates a separate inlet, filter pack, and pump assembly. Modules A, B, and C are equipped with 25 mm diameter filters and 2.5  $\mu\text{m}$  cyclones that allow for sampling of particles with aerodynamic diameters less than 2.5  $\mu\text{m}$  (PM<sub>2.5</sub>). The nominal flow rate for modules A, B, and C is 22.8 lpm (liter per minute), corresponding to 32.8  $\text{m}^3$  air volume over 24-hr. [Characterization](#) of the cut-point of the PM<sub>2.5</sub> sampler was reported by McDade et al. (2006). Module D is fitted with a PM<sub>10</sub> inlet to collect particles with aerodynamic diameters less than 10  $\mu\text{m}$ . The nominal flow rate for module D is 16.9 lpm, corresponding to 24.3  $\text{m}^3$  air volume over 24-hr. Each module contains a filter substrate specific to the planned chemical analysis (Figure 2). All analytical results are compiled by the laboratory<sup>1</sup> responsible for network operations and for initial processing and validation. Data are delivered to the Environmental Protection Agency (EPA) [Air Quality System](#) database and to the Cooperative Institute for Research in the Atmosphere (CIRA) [Federal Land Manager Environmental Database](#) (FED).

---

<sup>1</sup> The NPS contractors for the period of this guide are UC Davis for network operations, gravimetric mass, light absorption, and XRF; RTI for ion analysis; and DRI for carbon analysis.

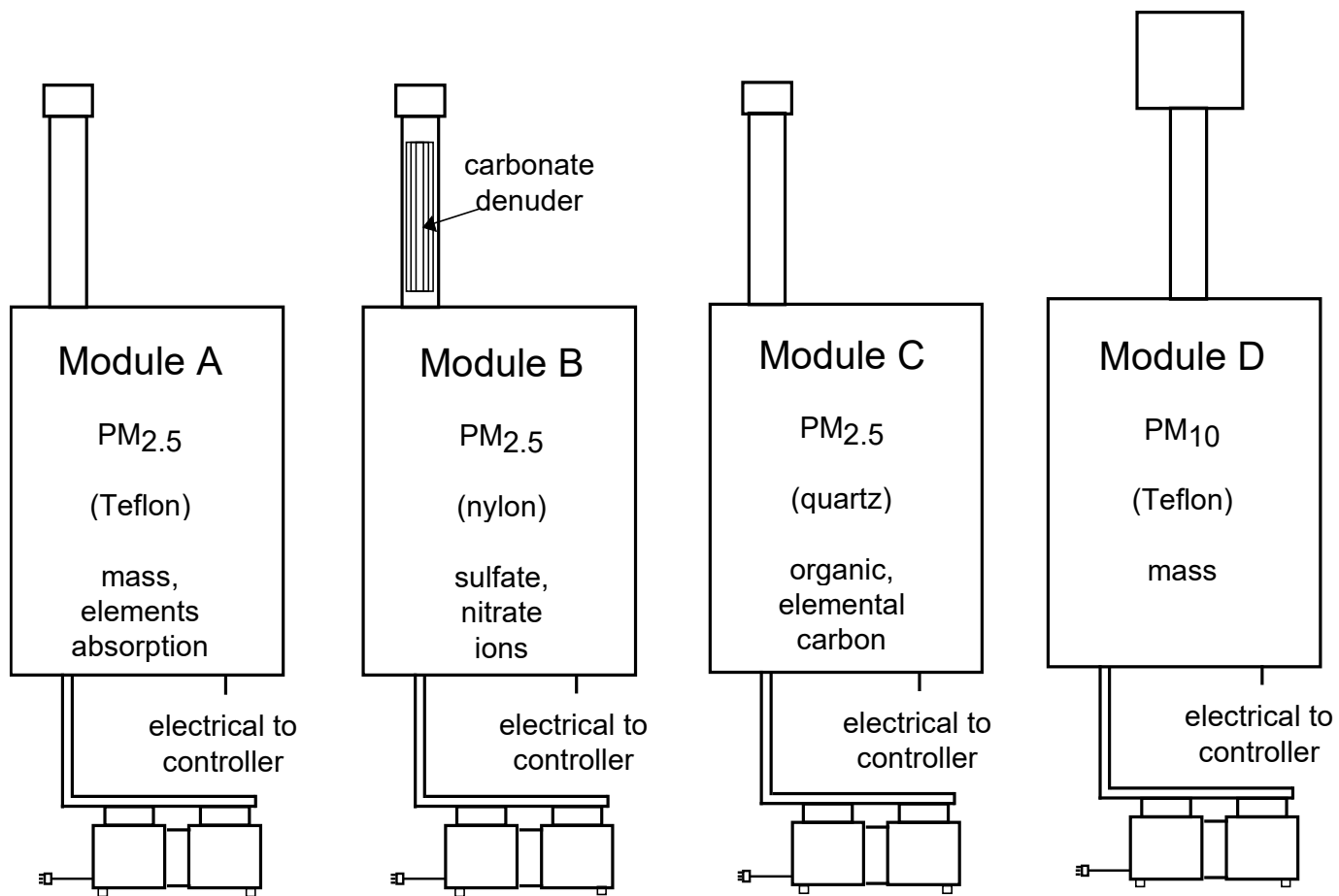


Figure 2. IMPROVE sampler showing the four modules with separate inlets and pumps. Substrates with analyses performed for each module are also shown.

Module A is equipped with a 25 mm diameter PTFE (polytetrafluoroethylene) Teflon® (referred to as “Teflon”) filter with a deposit area of 3.53 cm<sup>2</sup> (McDade et al., 2009). The filter is analyzed for PM<sub>2.5</sub> gravimetric fine mass (also referred to as fine mass, FM), elemental analysis, and filter light absorption. Samples are pre- and post-weighed to gravimetrically determine PM<sub>2.5</sub> fine mass using an electro-microbalance, after equilibrating for four hours at 30–40% relative humidity (RH) and 20–30° C. Module A Teflon filters are weighed in chambers with strict environmental controls, with the temperature set to 21.5 °C ± 1.0 °C and RH set to 39% ± 2.0%.

Elemental analysis is performed on the module A Teflon filters for elements with atomic number greater than 11 (Na) and less than 82 (Pb) by X-ray fluorescence (XRF), with a subset of elements reported. Starting in 2011 the XRF analysis has been performed with Malvern PANalytical Epsilon 5 instruments.

The filter light absorption coefficient ( $f_{abs}$ , Mm<sup>-1</sup>) is determined from the module A Teflon filter using a hybrid integrating plate/sphere system (HIPS) that shines a laser light (wavelength of 633 nm) on the backside of the filter and measures reflected and transmitted light to determine the light absorption by the PM<sub>2.5</sub> sample (White et al., 2016).

Module B is fitted with a sodium carbonate coated denuder tube in the inlet to remove gaseous nitric acid in the air sample, followed by a 37 mm diameter Nylasorb (nylon) filter as the collection substrate. The material collected on the nylon filter is extracted and subsequently analyzed for the anions sulfate, nitrate, nitrite, and chloride using ion chromatography (IC).

Module C uses a 25 mm diameter quartz fiber filter that is analyzed by thermal optical reflectance (TOR) for particulate organic and elemental carbon (OC and EC, respectively) (Chow et al., 1993). Thermally derived carbon fractions, including OC and EC, have been measured since 2016 using the DRI Model 2015 multiwavelength carbon analyzer (Chen et al., 2015; Chow et al., 2015). In this method, reflectance (R) from and transmittance (T) through a punch from the quartz filter are monitored continuously as the temperature is ramped through different steps that define the fractions. The evolved carbon at each temperature step is oxidized to carbon dioxide and quantified with a nondispersive infrared detector. R and T are monitored at 405, 445, 532, 635, 780, 808, and 980 nm wavelengths throughout the analysis to detect OC charring to EC from the aerosol deposit and organic vapors adsorbed throughout the quartz filter. Carbon that evolves after R returns to its initial value for the 635 nm wavelength in a 98% He/2% O<sub>2</sub> carrier gas is classified as EC in the aerosol deposit. The amount of carbon associated with charring during the process is referred to as OP. When the reflected or transmitted light returns to its original intensity, the pyrolyzed (charred) OP is assumed to have been removed. Temperature-defined fractions are 1) OC1, OC2, OC3, and OC4 that evolve in a pure He [>99.999%] atmosphere at 140, 280, 480, and 580 °C, respectively; and 2) EC1, EC2, and EC3 that evolve in a 98% He/2% O<sub>2</sub> atmosphere at 580, 740, and 840 °C, respectively). In addition to the carbon fractions, the following parameters are reported: 1) total organic carbon by reflectance (OC = OC1 + OC2 + OC3 + OC4 + OP); 2) total elemental carbon by reflectance (EC = EC1 + EC2 + EC3 - OP); 3) total carbon (TC): all carbon evolved from the filter punch between ambient (~25 °C) and 840 °C during analysis; and 4) laser signals, including initial, minimum, and final laser reflectance and transmittance value counts for each wavelength.

Finally, module D is fitted with a PM<sub>10</sub> inlet and uses a 25 mm diameter Teflon filter. PM<sub>10</sub> aerosol mass concentrations are determined gravimetrically, following a similar protocol as PM<sub>2.5</sub> gravimetric mass measurements.

Field blanks are collected to determine positive artifacts that are used to correct concentrations of all the reported species. Field blanks are collected randomly at all sites on a periodic basis. Field blanks are handled as normal filters (loaded into cassettes and cartridges, shipped to and from the field, and left in the sampler for a week) except no air is drawn through them ([SOP 351 Data Processing and Validation](#)).

Additional details regarding IMPROVE sampling and analysis can be found in the [IMPROVE VI report](#) (Hand et al., 2023).

#### 4.0 ACCESSING AND DOWNLOADING IMPROVE DATA FROM FED WEBSITE

The Federal Land Manager Environmental Database ([FED](#)) provides access to a number of environmental datasets, including IMPROVE, as well as many tools for analyzing air quality data. This section provides a guide for downloading IMPROVE speciated mass and extinction

data from FED. All users are encouraged to review the IMPROVE [data advisories](#) located on the IMPROVE website.

IMPROVE measured and calculated data can be downloaded from the [FED Query Wizard](#). The first page of the FED Query Wizard provides a list of datasets available for download, including IMPROVE data as well as other datasets (see Figure 3).

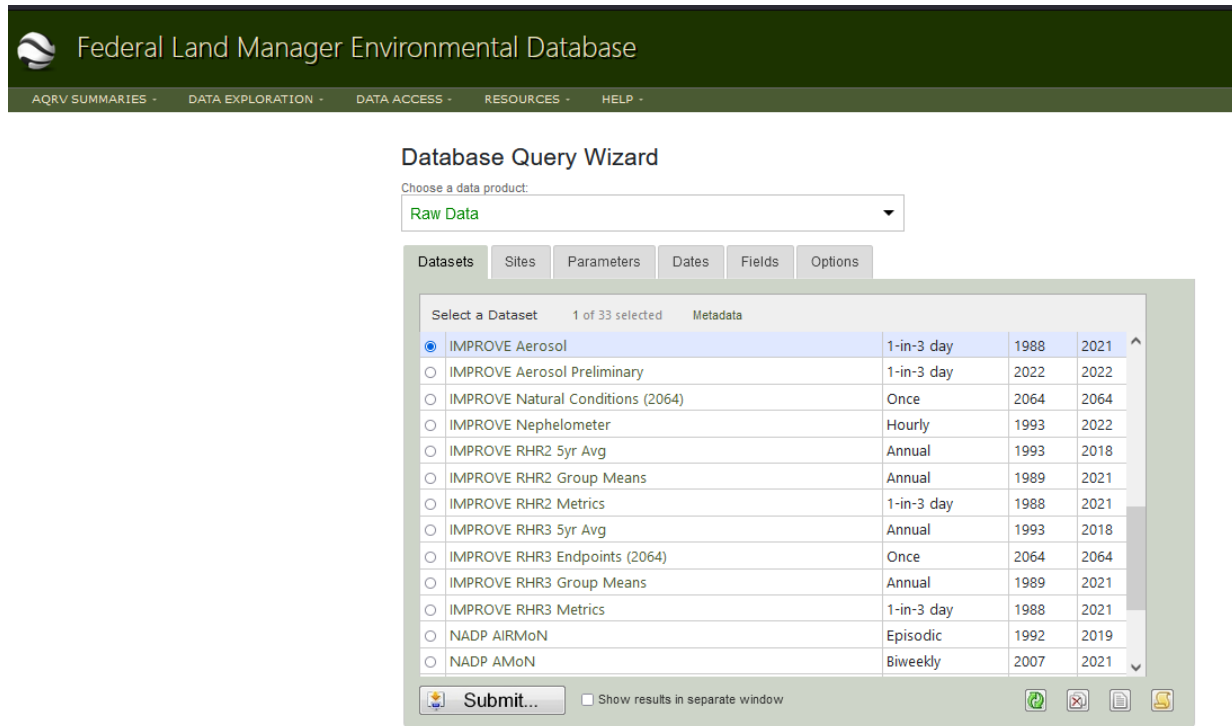


**Figure 3. FED Database Query Wizard page for downloading data.**

Several IMPROVE datasets are available for download, including daily and aggregated data under the “Datasets” tab of the Query Wizard. The tab includes a table with the dataset name, measurement or aggregation frequency, and the available dates. To select a dataset to download, click on the radio button on the left side of the dataset name. Clicking on the dataset name itself will open a window with site locations and other metadata. A list and description of the datasets are in Table B1 of Appendix B. Most of the IMPROVE datasets are associated with Regional Haze Rule (RHR) metrics and summaries and explanations of those datasets are available on the [RHR section](#) of the IMPROVE website. The rest of this discussion is focused on the “IMPROVE Aerosol” dataset which corresponds to the IMPROVE 24-hr validated (Level 3) mass dataset.

To choose the site(s) for download, click on the “Sites” tab, to the right of the “Datasets” tab. The “Sites” tab shows a list of sites that can be ordered by site name, site code, state, or available years by clicking on the headings for the Sites table. Individual sites or groups of sites can be selected by holding “control” and “shift”, respectively, while clicking on site names. All sites can be selected by clicking on “Select all” at the top. Clicking on “Metadata” provides a table of metadata for all the sites. After choosing sites, click on the “Parameters” tab, which lists

all of the available for download. A metadata table can be downloaded by clicking on “metadata”. See Table B2 in Appendix B for a list of parameters and descriptions.

After choosing desired parameters, the date range of the dataset can be selected from the “Dates” tab next to the “Parameters” tab. Dates can be chosen by year and month. The “Field” tab allows the selection of additional attributes for each data record. These attributes can include the site name, latitude and longitude, and the data minimum detection limits, uncertainties, and flags. The available field options are listed in Table B3 in Appendix B.

Finally, options for the downloaded data are found on the “Options” tab, where the user can select the output file types, formats, missing values and date formats. The option to download metadata as part of the data file, or in a separate file is also provided. Clicking “Submit” will create a dataset with the choices applied that is available for download. Clicking on the file name will open the data file as another window; right clicking on the file name will bring up a menu of options; “save link as” will download the file. The metadata also includes site location information, parameter description, site history, dataset history, and status flag definitions.

The flags available for download include those submitted from the data provider (Flag 1 and Flag 2) or those created during data import (Status Flag, Flag 3, and Flag 4). Status flags are listed in Table C1 in Appendix C. Flag 1 corresponds to the primary status, which is discussed in Section 6. Flag 2 corresponds to the site objective: RT (Routine) or CL (Collocated). Flag 3 corresponds to the sample module (A, B, C, or D), and Flag 4 corresponds to the Parameter Occurrence Code (POC), which is the same as the POC parameter (see Table B3).

## 5.0 DATA PROCESSING

The following is a description of the data processing routines used to convert the field and laboratory measurements to ambient concentrations. This information is reproduced from the IMPROVE [Standard Operating Procedure #351](#). Ambient concentrations are calculated from filter measurements and sample air volume. Artifact corrections are derived from field blanks. Field blanks are handled as normal filters (loaded into cassettes and cartridges, shipped to and from the field, and left in the sampler for a week) except that no air is drawn through them.

### *Volume*

The sample volume (V) is the product of the volumetric flow rate (Q) and the sampling duration ( $V = Q \times \text{Sample Duration}$ ). As stated earlier, the target nominal flow is 22.8 lpm for modules A, B, and C, and 16.9 lpm for module D. For a 24-hr sample, these flow rates lead to nominal volumes of 32.8 m<sup>3</sup> and 24.3 m<sup>3</sup>, for PM<sub>2.5</sub> and PM<sub>10</sub> samples, respectively. However, the flow rate can vary from day-to-day and over the sampling period; thus the measured flow rate is used to calculate V. A valid sample has a flow rate that remains within a defined bound of the nominal flow rate. Flow rates are audited to ensure that the nominal flow rate falls within 10% of a NIST (National Institute of Standards and Technology) certified device. [Technical system audits](#) are performed regularly within the network.

### *Concentration*

The concentration (C) is calculated using equation 1, where the mass of material on the filter is equal to the difference between the mass measured on the sample (A) and the artifact mass (B). For gravimetric analysis, B is determined from the pre-weight of individual Teflon filters. For measurement of ions, elements, and carbon, B is determined from the median of field blank loadings. For additional details, see [the SOP](#).

$$C = \frac{A-B}{V} \quad (1)$$

C is the ambient concentration ( $\mu\text{g m}^{-3}$ ), A is the mass measured on sample ( $\mu\text{g filter}^{-1}$  or  $\mu\text{g cm}^{-2}$  for XRF species), B is the artifact mass ( $\mu\text{g filter}^{-1}$  or  $\mu\text{g cm}^{-2}$  for XRF species), and V is the sample air volume in cubic meters. For XRF mass in units of  $\mu\text{g cm}^{-2}$ , a deposit envelope of  $3.53 \text{ cm}^2$  is used to calculate mass in  $\mu\text{g filter}^{-1}$ .

#### *Minimum Detection Limits and Artifacts*

An artifact is defined as any increase or decrease of material on the filter that positively or negatively biases the measurement of ambient concentration. Artifact corrections are applied to the ions, carbon, and element measurements by subtracting the median field blank. Field blanks are used to calculate representative network wide statistics that are used to perform artifact correction, estimate uncertainty, and calculate minimum detection limit (MDL). Artifact examples include:

1. Contamination of the filter medium (positive).
2. Contamination acquired by contact with the cassettes or in handling (positive).
3. Adsorption of gases during collection that are erroneously measured as particles (positive).
4. Volatilization of particles during collection and in handling (negative).
5. Fall-off of particles during handling after collection (negative).

For the ion and element measurements, the artifact correction method attempts to account for the first two types of artifacts and is estimated using data from field blanks. For the carbon measurements, the artifact correction method attempts to account for the first three types of artifacts and is estimated using data from field blanks. Measurements are not corrected for the two negative artifact types (volatilization and falloff).

During 2018 through 2020, IMPROVE data processing was modified to standardize field blank processing, uncertainty calculation, and MDL calculation across all analyses. These MDLs are reported with the data on FED. Prior to this period, the particulars of these estimates varied by analysis. There are now two standard calculation paths, one that is filter lot-specific for analyses that are dependent on filter lot variability and one that is independent of filter lot. The lot-specific analyses are XRF and filter light absorption, while gravimetric mass, IC, and TOR are lot-independent.

Artifact correction and MDL estimates are based on monthly field blank statistics, and reported uncertainty depends partly on the MDL estimate. For lot-independent analyses, a minimum of 50 field blanks is required to calculate the statistics, and a minimum of 35 field blanks is required for lot-specific analyses. In most cases, there are enough field blanks of each

lot within a month to meet these minimum requirements. However, if there are not, the algorithm includes field blanks from prior and/or subsequent months until the minimum threshold is reached. The two statistics calculated are median and 95<sup>th</sup> percentile. The general equation for calculating MDL is shown in equation 2; the equation may vary slightly depending on species (see [SOP](#) for more details):

$$mdl = \frac{\text{Max}(P95-B, \text{mdl}_{\text{analytical}})}{V} \quad (2)$$

P95 is the 95<sup>th</sup> percentile of field blank measurements ( $\mu\text{g filter}^{-1}$ ), B is the artifact mass,  $\text{mdl}_{\text{analytical}}$  is the analytical mdL and is reported from the analytical laboratory, and V is the sample volume ( $\text{m}^3$ ).

### *Uncertainty*

The uncertainty ( $\sigma(c)$ ) is reported on FED with each concentration. The general model for the uncertainty is a quadratic sum of two components of uncertainty as shown in equation 3.

$$\sigma(c) = \sqrt{[fC]^2 + \left[\frac{\sigma_a}{V}\right]^2} \quad (3)$$

The analytical uncertainty is given by  $\sigma_a$ . Analytical uncertainty is determined and reported by the laboratories. It is a constant term from additive sources of uncertainty, such as those related to background contamination of the filters. The sample air volume is V ( $\text{m}^3$ ), C is the ambient concentration ( $\mu\text{g m}^{-3}$ ), and  $f$  is the fractional uncertainty. Fractional uncertainty results from various sources of proportional uncertainties, such as analytical calibration and flow rate measurements, and is determined from collocated measurements. More details for calculating uncertainties can be found in the [SOP and Appendix D](#).

## 6.0 DATA VALIDATION

### 6.1 Definition of Primary Status Flags

Primary status flags (Flag 1 in Table C1 in Appendix C) are used as standardized abbreviations describing the status of individual sample results and are assigned during validation processes (Table C2). Samples associated with “Terminal” flags are invalidated for a variety of reasons, and no concentration, uncertainty, or MDL values are reported, whereas those associated with “Informational” flags are still valid samples and concentrations, uncertainties, and MDLs are reported. The “Temporary” flags occur in the Preliminary dataset and are used to aid data validation. They are replaced before final data reporting.

### 6.2 Flow Validation

The criteria for flags that denote clogged filters, clogging filters, or incorrect flow rates are determined based on calculation limitations, performance testing, and particle size cut. Incorrect flow rates affect the PM<sub>2.5</sub> cyclone particle size cut point. The criteria for applying CL (clogged filter), CG (clogging filter) and LF (incorrect flow) flags are based primarily on cut point characterization of the PM<sub>2.5</sub> cyclone with the size range between 2.25  $\mu\text{m}$  – 2.75  $\mu\text{m}$

considered reasonable for data labeled as PM<sub>2.5</sub>. Note that at the nominal flow rate of 23 lpm for the PM<sub>2.5</sub> cyclone, the 50% cutoff diameter is 2.36  $\mu\text{m}$  rather than 2.5  $\mu\text{m}$ . At flow rates of 15 lpm, 18 lpm, 19.7 lpm, and 24.1 lpm, the cyclone cut point is 3.6  $\mu\text{m}$ , 3.0  $\mu\text{m}$ , 2.75  $\mu\text{m}$ , and 2.25  $\mu\text{m}$ , respectively.

A filter is considered clogged and flagged as CL if the flow rate is less than 15 lpm for more than 6 hours or the average flow rate is less than 15 lpm. Similarly, a clogging filter sample has the flag CG, and has flow rates less than 18 lpm for more than 6 hours or an average flow rate less than 18 lpm. A filter sample is flagged as LF when it has a low or high flow rate defined as the average flow rate  $< 19.7$  lpm or  $> 24.1$  lpm, respectively. CL is a terminal flag, while CG and LF flags are informational only. The relationship between the PM<sub>10</sub> Sierra cyclone and particle size cut is not well characterized so the criteria are determined somewhat arbitrarily, which are defined in Table C3 in Appendix C. It is important to note that under the circumstance of a failing pump that produces less vacuum, the calculated flow rates for the PM<sub>10</sub> module are not valid.

The IMPROVE sampler can clog under conditions of heavy aerosol loading, such as in dense wildfire smoke or dust storms. Beginning with select sites in late 2022, the IMPROVE sampler controller software was upgraded to allow for automatic cutoff when flow rates were measured below a critical threshold for more than 15 continuous minutes. This was to preserve samples with a known sampling volume to retain valid concentration calculations even if sample duration is short. Prior to this change, these samples would have been flagged CG and reported with no concentration. Now, if the elapsed time is less than 18 hours, these samples are flagged as SD (for short-duration sample) and reported with a calculated concentration and their elapsed time. SD samples are not valid for RHR calculations, but are provided to the community for other uses. The automatic cutoff software is expected to be deployed to the entire network by 2024.

## 7.0 CALCULATED MASS VARIABLES (IMPROVE REPORT VI)

Algorithms for calculating variables derived from IMPROVE data are provided below. These algorithms are used to calculate speciated and reconstructed fine mass and were applied in the [IMPROVE Report VI](#) (Hand et al., 2023). In some cases these algorithms may differ from those used to determine calculated variables in the FED database, such as RHR metrics, and will be noted as such. All units are in  $\mu\text{g m}^{-3}$  unless otherwise noted.

### ***PM<sub>2.5</sub> Ammonium Sulfate***

Sulfate is assumed to be fully neutralized as ammonium sulfate (ammSO<sub>4</sub>). AmmSO<sub>4</sub> can be calculated from sulfur (S, derived from X-ray fluorescence, XRF) or sulfate ion concentrations (equation 4). Because of issues related to varying biases in sulfur derived from XRF (White, 2007a; 2009), sulfate is used to calculate ammSO<sub>4</sub>. After 1 May 1995, missing sulfate samples are replaced by  $3 \times S$  (to account for additional oxygen molecules). Before 1995 no substitutions of S were used because of underestimations of S due to masked filters (Schichtel, 2003). Before 2011, values of S below the MDL are replaced with  $0.5 \times \text{MDL}$ . After 2011 (when the PANalytical XRF began use), no replacements below the MDL are made. The

molar correction factor (mcf) of 1.375 is determined by the ratio of the molecular weight of ammSO<sub>4</sub> to sulfate ion; similarly, a factor of 4.125 is used to convert sulfur to ammSO<sub>4</sub>.

$$\text{AmmSO}_4 = 1.375 \times [\text{sulfate ion}] \quad (4)$$

### ***PM<sub>2.5</sub> Ammonium Nitrate***

Nitrate is assumed to be in the form of ammonium nitrate (ammNO<sub>3</sub>, equation 5). During 1996-2000 wintertime nitrate concentrations were determined to be anomalously low and a data advisory was issued. An in-depth investigation identified several sites that were influenced but no cause was discovered (McDade, 2007; Debell, 2006). Based on these issues, nitrate data are not used during this period.

$$\text{AmmNO}_3 = 1.29 \times [\text{nitrate ion}] \quad (5)$$

### ***PM<sub>2.5</sub> Organic Carbon***

Organic carbon (OC) is the sum of carbon sub-fractions from thermal optical reflectance measurements (equation 6). OC1, OC2, OC3, and OC4 correspond to carbon fractions determined at different temperature profiles of the IMPROVE\_A protocol measurement (see Chow et al., 2015). OP corresponds to the carbon fraction associated with charring or pyrolyzing during the measurement (Chow et al., 2004).

$$\text{OC} = \text{OC1} + \text{OC2} + \text{OC3} + \text{OC4} + \text{OP} \quad (6)$$

If OC concentrations are calculated to be less than -1  $\mu\text{g m}^{-3}$  they are set -999.

### ***PM<sub>2.5</sub> Particulate Organic Matter***

Organic matter from carbon (OMC, also referred to as particulate organic matter, POM) is calculated from OC data by multiplying the OC concentrations by an assumed ratio of organic mass (OM) to OC (OM/OC) (equation 7). OMC accounts for atoms other than carbon in organic matter. OMC as reported in FED is calculated using a constant OM/OC of 1.8. However, for the IMPROVE [Report VI](#) (Hand et al., 2023), a monthly-varying OM/OC is used (Table 1). More information can be found in the IMPROVE Report VI.

$$\text{OMC} = (\text{OM/OC}) \times [\text{OC}] \quad (7)$$

**Table 1. Monthly values of the organic mass to organic carbon ratio (OM/OC).**

Month	OM/OC
Jan	1.5
Feb	1.5
Mar	1.5
Apr	1.6
May	1.7
Jun	1.9
Jul	2.0
Aug	2.1

Sept	2.0
Oct	1.7
Nov	1.7
Dec	1.7
Annual	1.7

### ***PM<sub>2.5</sub> Elemental Carbon***

Elemental carbon (EC) is the sum of carbon sub fractions from thermal optical reflectance measurements (equation 8). EC1, EC2, and EC3 correspond to carbon fractions determined at different temperature profiles of the IMPROVE\_A protocol measurement (see Chow et al., 2015). OP corresponds the carbon fraction associated with charring or pyrolyzing during the OC measurement (Chow et al., 2004).

$$\text{EC} = \text{EC1} + \text{EC2} + \text{EC3} - \text{OP} \quad (8)$$

If EC concentrations are calculated to be less than  $-1 \text{ } \mu\text{g m}^{-3}$  they are set to -999.

### ***PM<sub>2.5</sub> Total Carbon***

Total Carbon (TC) is the sum of OC and EC ( $\text{TC} = \text{OC} + \text{EC}$ ).

### ***PM<sub>2.5</sub> Soil or Fine Dust***

Soil, or fine dust, is calculated using elemental species data from XRF analysis. Elemental concentrations are multiplied by factors assuming normal oxides of elemental species associated with crustal material (equation 9, following Malm et al., 1994).

$$\text{Soil} = 2.53 \times [\text{Al}] + 2.86 \times [\text{Si}] + 1.87 \times [\text{Ca}] + 2.78 \times [\text{Fe}] + 2.23 \times [\text{Ti}] \quad (9)$$

Soil values downloaded from FED are calculated using the original soil formula from Malm et al. (1994). However, for the IMPROVE Report VI the multipliers in the soil equation were increased by 15% (as reflected in equation 9) based on multiple linear regression results by Hand et al. (2019) that suggested that soil was under predicted by the original algorithm. For XRF measurements before 2011, values below MDLs are substituted with  $0.5 \times \text{MDL}$ . Data for each species must be valid for a valid soil estimate.

### ***PM<sub>2.5</sub> Sea Salt***

Sea salt is calculated using chloride ion data and a mass correction factor of 1.8 (equation 10; SS is 55% NaCl by weight).

$$\text{Sea salt} = 1.8 \times [\text{chloride ion}] \quad (10)$$

When chloride ion data are missing, chlorine data from XRF are substituted. Before 2011 chlorine data below MDL are substituted with  $0.5 \times \text{MDL}$ .

### ***Coarse Mass***

Coarse mass (CM) is the difference between gravimetric PM<sub>10</sub> and PM<sub>2.5</sub> mass concentrations (equation 11). If calculated CM is less than -1  $\mu\text{g m}^{-3}$  it is set to -999 (missing value).

$$\text{CM} = \text{PM}_{10} - \text{PM}_{2.5} \quad (11)$$

### ***Reconstructed Fine Mass***

Reconstructed fine mass (RCFM) is the sum of the above PM<sub>2.5</sub> species (equation 12). All of the species are required to be valid for valid RCFM.

$$\text{RCFM} = \text{AmmSO}_4 + \text{AmmNO}_3 + \text{OMC} + \text{EC} + \text{Soil} + \text{Sea salt} \quad (12)$$

### ***Reconstructed Total Mass (RCTM)***

Reconstructed total mass is the sum of PM<sub>2.5</sub> species and CM (equation 13). All of the species are required to be valid for valid RCTM.

$$\text{RCTM} = \text{AmmSO}_4 + \text{AmmNO}_3 + \text{OMC} + \text{EC} + \text{Soil} + \text{Sea salt} + \text{CM} \quad (13)$$

## **8.0 RECONSTRUCTED LIGHT EXTINCTION COEFFICIENTS**

### **8.1 IMPROVE Report VI**

Algorithms for calculating light extinction coefficients ( $b_{\text{ext}}$ ) using speciated IMPROVE mass data are provided below. A modified IMPROVE reconstruction extinction equation was used to calculate light extinction coefficients for the [IMPROVE VI report](#) (equation 14). This algorithm differs from the algorithm applied by the Regional Haze Rule (see section 8.2).

$$\begin{aligned} b_{\text{ext}} = & 3 \times f(\text{RH}) \times [\text{AmmSO}_4] + 3 \times f(\text{RH}) \times [\text{AmmNO}_3] + \\ & 4 \times [\text{OMC}] + 10 \times [\text{EC}] + 1 \times [\text{Soil}] + 1.7 \times f(\text{RH})_{\text{ss}} \times [\text{Sea Salt}] + \\ & 0.6 \times [\text{CM}] + \text{site-specific Rayleigh scattering} \end{aligned} \quad (14)$$

The units of  $b_{\text{ext}}$  and Rayleigh scattering are in inverse megameters ( $\text{Mm}^{-1}$ ). Mass concentrations (in brackets) of aerosol species are in units of  $\mu\text{g m}^{-3}$ , and dry mass extinction efficiencies have units of  $\text{m}^2 \text{ g}^{-1}$ . Mass extinction efficiencies of  $3 \text{ m}^2 \text{ g}^{-1}$  were used for both ammSO<sub>4</sub> and ammNO<sub>3</sub>,  $4 \text{ m}^2 \text{ g}^{-1}$  for OMC,  $10 \text{ m}^2 \text{ g}^{-1}$  for EC,  $1 \text{ m}^2 \text{ g}^{-1}$  for soil,  $1.7 \text{ m}^2 \text{ g}^{-1}$  for sea salt, and  $0.6 \text{ m}^2 \text{ g}^{-1}$  for CM. These values correspond to a wavelength of 550 nm (Hand and Malm, 2007; Pitchford et al., 2007). Site-specific Rayleigh scattering values are on the [IMPROVE website](#).

The  $f(\text{RH})$  values applied in equation 14 account for enhanced scattering due to higher relative humidity (RH) environments and were computed using the algorithm outlined in the Regional Haze Rule [Guidelines](#) for Tracking Progress (EPA, 2003). The  $f(\text{RH})$  curve was calculated with Mie theory, assuming a lognormal ammSO<sub>4</sub> mass size distribution with a geometric mass mean diameter of 0.3  $\mu\text{m}$  and a geometric standard deviation of 2.0 and

interpolated between the deliquescence and efflorescence points. This  $f(RH)$  was applied to both ammSO<sub>4</sub> and ammNO<sub>3</sub> (see Figure 4a). The  $f(RH)_{ss}$  curve applied to sea salt was computed assuming a sea salt geometric mass mean diameter of 2.5  $\mu\text{m}$  and a geometric standard deviation of 2 and is shown in Figure 4b and values are available on the IMPROVE algorithm [section](#) of the IMPROVE website (Pitchford et al., 2007). Below the deliquescence point (RH = 47%) the  $f(RH)_{ss}$  is set to 1. POM was assumed to be nonhygroscopic. Humidification factors are unitless.

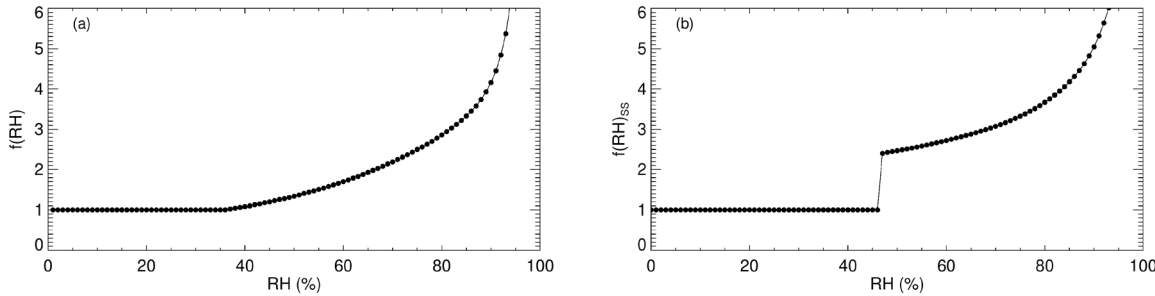


**Figure 4. (a) Humidification factors ( $f(RH)$ ) as a function of relative humidity (RH, %) for ammSO<sub>4</sub>. A lognormal mass size distribution with a geometric mass mean diameter of 0.3  $\mu\text{m}$  and a geometric standard deviation of 2.0 was assumed. (b)  $f(RH)_{ss}$  for sea salt with an assumed lognormal mass size distribution with a geometric mass mean diameter of 2.5  $\mu\text{m}$  and a geometric standard deviation of 2.0. A wavelength of 550 nm was used.**

RH is not routinely measured at most IMPROVE sites. To calculate visibility metrics, monthly and site-specific  $f(RH)$  curves were generated based on monthly climatological mean RH values. These monthly RH values eliminate the effects of interannual variations in RH while maintaining typical regional and seasonal humidity patterns around the United States. The EPA produced recommended monthly  $f(RH)$  values for each CIA, based on analysis of a 10-year record (1988–1997) of hourly RH data from 292 National Weather Service stations across the 50 states and the District of Columbia, as well as from 29 IMPROVE and IMPROVE-protocol monitoring sites, 48 Clean Air Status and Trends Network (CASTNet) sites, and 13 additional sites administered by the National Park Service. Values of  $f(RH)$  for all locations were generated using an interpolation scheme with an inverse distance weighting [technique](#) (EPA, 2001). The daily ambient ammSO<sub>4</sub>, ammNO<sub>3</sub>, and sea salt extinction coefficients for each site can be calculated using these values which are available on the [IMPROVE website](#).

Visual range and extinction measurements are nonlinear with respect to human perception of visual scene changes caused by haze. The deciview (dv) haze index was derived with a number of assumptions such that uniform changes in haze correspond to approximately uniform incremental changes in visual perception (Pitchford and Malm, 1994). Deciview is calculated from reconstructed  $b_{\text{ext}}$ , using equation 15:

$$dv = 10 \times \ln(b_{\text{ext}}/10) \quad (15)$$

In the original IMPROVE equation (Malm et al., 1994),  $dv = 0$  for pristine (Rayleigh scattering) conditions (elevation  $\sim 1.8$  km) for elevations where Rayleigh scattering = 10  $\text{Mm}^{-1}$ . For different values of site-specific Rayleigh scattering, as specified in equations 14 and 15, it is possible to have a negative dv for pristine conditions ( $b_{\text{ext}} < 10 \text{ Mm}^{-1}$ ).

## 8.2 Regional Haze Rule Metrics

The Regional Haze Rule (RHR) guidelines include a separate reconstruction extinction algorithm (often referred to as the “second” IMPROVE equation) that assumes a bimodal distribution and size-mode dependent mass scattering efficiencies (Pitchford et al., 2007). The algorithm for calculating the extinction coefficient using RHR guidelines ( $b_{ext\_RHR}$ ) is provided in equation 16:

$$\begin{aligned} b_{ext\_RHR} = & 2.2 \times f_S(RH) \times [AmmSO_4]_S + 4.8 \times f_L(RH) \times [AmmSO_4]_L + \\ & 2.4 \times f_S(RH) \times [AmmNO_3]_S + 5.1 \times f_L(RH) \times [AmmNO_3]_L + \\ & 2.8 \times [OMC]_S + 6.1 \times [OMC]_L + \\ & 10 \times [EC] + 1 \times [Soil] + 1.7 \times f(RH)_{ss} \times [Sea\ salt] + 0.6 \times [CM] + \\ & \text{site-specific Rayleigh scattering} + 0.33 \times [NO_2(ppb)] \end{aligned} \quad (16)$$

where the units of  $b_{ext\_RHR}$  and Rayleigh scattering are given in  $Mm^{-1}$ . Concentrations are shown in brackets ( $\mu\text{g m}^{-3}$ ) and separated into small (subscript of “S”) and large (“L”) modes for  $ammSO_4$ ,  $ammNO_3$ , and OMC based on their mass. For masses less than  $20 \mu\text{g m}^{-3}$ , the fraction in the large mode is estimated by dividing the total concentration of the component by  $20 \mu\text{g m}^{-3}$ . For example, if the total OMC concentration is  $4 \mu\text{g m}^{-3}$ , the fraction in the large mode is calculated as  $4/20 = 1/5$  of  $4 \mu\text{g m}^{-3} = 0.8 \mu\text{g m}^{-3}$ ; the remaining  $3.2 \mu\text{g m}^{-3}$  is in the small mode. If the total concentration of a component exceeds  $20 \mu\text{g m}^{-3}$ , all of it is assumed to be in the large mode. The small and large modes of  $ammSO_4$  and  $ammNO_3$  have associated hygroscopic growth curves,  $f_S(RH)$  and  $f_L(RH)$ , respectively, while  $f_{ss}(RH)$  is the hygroscopic growth curve for sea salt. Dry mass extinction efficiency terms are in units of meters squared per gram ( $\text{m}^2 \text{g}^{-1}$ ); and the hygroscopic growth terms,  $f(RH)$ , are unitless. Values of  $f(RH)$  are on the [IMPROVE website](#). Light absorption by nitrogen dioxide ( $NO_2$ ) is included if data are available (Pitchford et al., 2007).

Speciated mass concentrations are calculated similarly in equation 16, except for the following:  $ammSO_4$  is calculated from sulfur data ( $AmmSO_4 = 4.125 \times S$ ), OMC uses an OM/OC ratio of 1.8, and soil has no 15% increase (see Malm et al., 1994).

## 9.0 DATA USAGE

Changes in sampling protocols, analytical techniques, or data issues can affect data usage. As such, data advisories and quality assurance reports are routinely provided.

### *Data Advisories*

Data advisories are provided on the [IMPROVE website](#) and data users are encouraged to check it regularly to discover data anomalies, potential problems, and new uses for IMPROVE data. The advisories are not meant to be comprehensive or complete. In addition, unless explicitly stated, the data advisories are not necessarily endorsed by the IMPROVE Steering Committee or the National Park Service.

### *Quality Assurance/Quality Control (QA/QC) reports*

The IMPROVE monitoring program has a rigorous quality assurance program and extensive quality control and assessment procedures. Primary documents governing the QA program, as well as presentations aimed at [QA and QC measures](#) can be found on the IMPROVE website.

### *Publications*

For data inclusion in journal publications, the following suggestions are encouraged:

- Please inform Bret Schichtel (Bret.Schichtel@colostate.edu) of the planned publication. Drafts of publications will be reviewed upon request for issues that could affect the data interpretation.
- Preferred Reference: Please reference the Malm, et al. (1994) article when using IMPROVE data: Malm, W. C., J. F. Sisler, D. Huffman, R. A. Eldred, and T. A. Cahill (1994), Spatial and seasonal trends in particle concentration and optical extinction in the United States, *J. Geophys. Res.*, 99, 1347-1370, doi: <https://doi.org/10.1029/93JD02916>.
- Preferred Acknowledgment: IMPROVE is a collaborative association of state, tribal, and federal agencies, and international partners. US Environmental Protection Agency is the primary funding source, with contracting and research support from the National Park Service. The Air Quality Group at the University of California, Davis is the central analytical laboratory, with ion analysis provided by Research Triangle Institute, and carbon analysis provided by Desert Research Institute.

## **10. TRENDS**

The IMPROVE network has been operating since 1988 and over these decades changes in analytical methods have occurred. Many of these changes are reported as [Data Advisories](#). Some of the changes that may affect trends in various species are described here.

Sulfur calibration issues have been reported over time (White, 2007a; 2009). In addition, before 1995, filters were masked and could result in an underestimation of sulfur concentrations (Schichtel, 2003).

During the late 1990s, IMPROVE nitrate ion concentrations at many sites fell below historical values during winter months. Investigations into the period from 1996 through 2000 revealed lower than usual concentrations during winter months, and the cause remains unknown (McDade, 2004; 2007; Debell, 2006). Concentrations returned to normal levels after 2000, after which the data were deemed valid.

OC and EC on quartz filters have been measured by DRI since 1987, starting with laboratory analyzers developed at the Oregon Graduate Institute (OGI, now part of the Oregon Health and Science University). By the late 1990s it was evident that the DRI/OGC analyzers were deteriorating. Some components were no longer manufactured, and the data acquisition system was antiquated. The Model 2001 (Atmoslytic Inc., Calabasas, CA) analyzer was developed and made commercially available as a replacement. It introduced a number of enhancements, including better characterization of sample temperature and sample atmosphere, automatic sample positioning, more rapid temperature response, improved seals and flow

control, greater heating capacity, advanced electronics, modern data acquisition, the potential for an automated sample changer, and the ability to simultaneously measure reflectance and transmittance. Concurrent with the hardware modifications was the application of a new TOR protocol, named IMPROVE\_A, designed to reflect the more accurate and less variable temperature and sample atmosphere conditions provided by the new instruments.

The Model 2001 analyzer was used for routine analysis of IMPROVE samples collected on or after 1 January 2005. Extensive testing prior to deployment had suggested that observable differences in the data record would be minimal (Chow et al., 2005). However, subsequent examination of data from the first two years of analysis (2005 and 2006) revealed unforeseen differences between data from the old and new instruments (White, 2007b). The differences vary as a function of site, but the new data generally identify a higher proportion of TC as EC and a lower proportion as OC than were observed in the final years of the old instruments. The EC/OC distinction is operationally defined, and the differences are not fully understood (White, 2007b).

Samples acquired after 1 January 2016 have been analyzed with the Model 2015 multiwavelength carbon analyzer (McGee Scientific Instruments, Berkeley, CA). Trends in OC and EC may be affected by changes in analytical methods. A recent review of carbonaceous measurements in the IMPROVE program identified shifts in analytical methods and their impacts on the fraction of EC to total carbon ( $TC = OC + EC$ ), i.e., EC/TC (Schichtel et al., 2021). One such shift occurred with hardware upgrades in 2005 that resulted in changes in the split between OC and EC that introduced uncertainty to trend analyses (Chow et al., 2007; White, 2007b). Other shifts in EC/TC have also occurred over the history of the program due to new analyzers, new calibrations, and undetermined reasons.

EC trends are affected by hardware and analytic changes, similar to issues that affect OC trends. In addition, Malm et al. (2020) suggested EC may be inadvertently and incorrectly assigned to the OC fraction during the thermal optical reflectance analysis, resulting in an underestimate of true EC concentrations. As discussed by Schichtel et al. (2021), EC concentrations have decreased at rural sites to the point that many sites have concentrations that are below the lower quantifiable limits (LQL, defined as  $3 \times MDL$ ). From 2017 to 2019, about 30% of all EC concentrations were below the LQL. More sites in the West were below LQL than in the East. These low concentrations make tracking trends difficult, especially for the 10<sup>th</sup> percentile concentrations.

Soil concentrations are determined by combining the oxides of elemental mass concentrations of Al, Si, Ca, Fe, and Ti. The analytical methods used to determine these species have evolved over time and included PIXE (proton induced X-ray emission) and XRF (X-ray fluorescence) techniques. The transitions from PIXE to XRF methods, the change in XRF anodes from Mo to Cu, as well as different calibration procedures affect the data by changing MDLs (Hyslop et al., 2015; Spada et al., 2023). In 2011, the analysis method switched to the PANalytical XRF system that resolved issues related to undetected Al with concentrations above the MDL (White, 2006). Changes in analytical methods may not equally affect data for each FD species; therefore, the integrated dust concentration may be less susceptible to possible variability introduced by the analytical methods, although this has not been specifically demonstrated.

Chloride ion data have been associated with negative biases from 2007 to 2011 due to elevated chloride mass loadings on nylon filter field blanks (Zhang, 2019).

Filter light absorption measurements have been performed with the HIPS method since 1994; however, data prior to 2003 were not properly calibrated because field blanks for these data were not available (White, 2015; 2016).

From December 2010 through September 2018, IMPROVE PM<sub>2.5</sub> and PM<sub>10</sub> gravimetric mass measurements were performed manually in a temperature-controlled laboratory using Mettler-Toledo XP6 microbalances. Prior to 2011, periodic laboratory measurements suggested that RH was typically below 50%; however, a laboratory relocation in 2011 resulted in highly variable RH conditions in the weighing laboratory. Laboratory RH was not continuously recorded, but available data suggest that RH varied significantly during weighing and since 2011 exceeded 40% for almost half of the analyses, occasionally exceeding 60% (White, 2016). Thus, from 2011 to 2018, gravimetric mass data were potentially subject to high RH conditions and likely contained particle-bound water (Hand et al., 2019). Beginning with samples and field blanks collected in October 2018, UC Davis transitioned from manual weighing to the Measurement Technology Laboratories (MTL) AH500E climate-controlled automated weighing system. The MTL AH500E system was used for the vast majority of the mass measurements from 2019 through 2020, although occasionally the system failed and the samples had to be weighed manually.

## 11. REFERENCES

Chen, L.-W., J. Chow, X. Wang, J. Robles, B. Sumlin, D. Lowenthal, R. Zimmermann, and J. Watson (2015), Multi-wavelength optical measurement to enhance thermal/optical analysis for carbonaceous aerosol, *Atmospheric Measurement Techniques*, 8(1), 451-461, doi:doi:10.5194/amt-8-451-2015.

Chow, J. C., J. G. Watson, L. C. Pritchett, W. R. Pierson, C. A. Frazier, and R. G. Purcell (1993), The DRI thermal/optical reflectance carbon analysis system: description, evaluation and applications in US air quality studies, *Atmospheric Environment. Part A. General Topics*, 27(8), 1185-1201, doi:https://doi.org/10.1016/0960-1686(93)90245-T.

Chow, J. C., J. G. Watson, L.-W. A. Chen, W. P. Arnott, H. Moosmüller, and K. Fung (2004), Equivalence of elemental carbon by thermal/optical reflectance and transmittance with different temperature protocols, *Environmental Science & Technology*, 38(16), 4414-4422, doi:10.1021/es034936u.

Chow, J. C., J. G. Watson, L.-W. A. Chen, M. Chang, and G. Paredes-Miranda (2005), Comparison of the DRI/OGC and Model 2001 Thermal/Optical carbon analyzers, *Prepared for IMPROVE Steering Committee, Fort Collins, CO, by Desert Research Institute, Reno, NV*, [http://vista.cira.colostate.edu/improve/Publications/GrayLit/013\\_CarbonAnalyzer/IMPROVE\\_CarbonAnalyzerAssessment.pdf](http://vista.cira.colostate.edu/improve/Publications/GrayLit/013_CarbonAnalyzer/IMPROVE_CarbonAnalyzerAssessment.pdf).

Chow, J. C., J. G. Watson, L.-W. A. Chen, M. O. Chang, N. F. Robinson, D. Trimble, and S. Kohl (2007), The IMPROVE\_A temperature protocol for thermal/optical carbon analysis:

maintaining consistency with a long-term database, *Journal of the Air & Waste Management Association*, 57(9), 1014-1023, doi:<https://doi.org/10.3155/1047-3289.57.9.1014>.

Chow, J. C., X. Wang, B. J. Sumlin, S. B. Gronstal, L.-W. A. Chen, D. L. Trimble, S. D. Kohl, S. R. Mayorga, G. Riggio, and P. R. Hurbain (2015), Optical calibration and equivalence of a multiwavelength thermal/optical carbon analyzer, *Aerosol and Air Quality Research*, 15(4), 1145-1159, doi:[doi:10.4209/aaqr.2015.02.0106](https://doi.org/10.4209/aaqr.2015.02.0106).

Debell, L. J. (2006), Data Validation Historical Report NO3,  
[http://vista.cira.colostate.edu/improve/wp-content/uploads/2022/09/044\\_Historical\\_QA\\_Report\\_Nitrate.pdf](http://vista.cira.colostate.edu/improve/wp-content/uploads/2022/09/044_Historical_QA_Report_Nitrate.pdf)

EPA, U. S. (2001), Interpolating relative humidity weighting factors to calculate visibility impairment and the effects of IMPROVE monitor outliers, 68-D-98-113, WA No. 3-39,  
<http://vista.cira.colostate.edu/Improve/wp-content/uploads/2016/03/DraftReportSept20.pdf>

EPA, U. S. (2003), Guidance for tracking progress under the Regional Haze Rule, *EPA-454/B-03-004*, <https://www.epa.gov/sites/default/files/2021-03/documents/tracking.pdf>

Hand, J. L., and W. Malm (2007), Review of aerosol mass scattering efficiencies from ground-based measurements since 1990, *Journal of Geophysical Research: Atmospheres*, 112(D16), 203, doi:[doi:10.1029/2007JD008484](https://doi.org/10.1029/2007JD008484).

Hand, J. L., A. J. Prenni, B. A. Schichtel, W. C. Malm, and J. C. Chow (2019), Trends in remote PM2.5 residual mass across the United States: Implications for aerosol mass reconstruction in the IMPROVE network, *Atmospheric Environment*, 203, 141-152,  
doi:[doi:10.1016/j.atmosenv.2019.01.049](https://doi.org/10.1016/j.atmosenv.2019.01.049).

Hand, J. L., et al. (2023), IMPROVE (Interagency Monitoring of Protected Visual Environments): Spatial and seasonal patterns and temporal variability of haze and its constituents in the United States Report VI, *CIRA Report*, 6.  
<http://vista.cira.colostate.edu/Improve/spatial-and-seasonal-patterns-and-temporal-variability-of-haze-and-its-constituents-in-the-united-states-report-vi-june-2023/>

Hyslop, N. P., K. Trzepla, and W. H. White (2015), Assessing the suitability of historical PM2.5 element measurements for trend analysis, *Environmental Science & Technology*, 49(15), 9247-9255, doi:DOI: 10.1021/acs.est.5b01572.

Malm, W. C., J. F. Sisler, D. Huffman, R. A. Eldred, and T. A. Cahill (1994), Spatial and seasonal trends in particle concentration and optical extinction in the United States, *Journal of Geophysical Research: Atmospheres*, 99(D1), 1347-1370, doi:  
<https://doi.org/10.1029/93JD02916>.

Malm, W., J. F. Sisler, M. Pitchford, M. Scruggs, R. B. Ames, S. Copeland, K. Gebhart, and D. Day (2000), IMPROVE (Interagency Monitoring of Protected Visual Environments): Spatial and seasonal patterns and temporal variability of haze and its constituents in the United States: Report III, *CIRA Report*, 3, <http://vista.cira.colostate.edu/Improve/spatial-and-seasonal-patterns-and-temporal-variability-of-haze-and-its-constituents-in-the-united-states-report-iii/>

Malm, W., B. Schichtel, J. Hand, and A. Prenni (2020), Implications of organic mass to carbon ratios increasing over time in the rural United States, *Journal of Geophysical Research: Atmospheres*, 125(5), e2019JD031480.

McDade, C. (2004), Summary of IMPROVE nitrate measurements, [http://vista.cira.colostate.edu/improve/Publications/GrayLit/025\\_IMPROVENitrate/Nitrate%20Summary\\_1004.pdf](http://vista.cira.colostate.edu/improve/Publications/GrayLit/025_IMPROVENitrate/Nitrate%20Summary_1004.pdf)

McDade, C. (2006), IMPROVE Particle Monitoring Network: Status Report to IMPROVE Steering Committee, in *2006 IMPROVE Steering Committee*, edited, Mammoth Cave National Park, [http://vista.cira.colostate.edu/Improve/wp-content/uploads/2016/04/UCDStatus0906\\_McDade.pdf](http://vista.cira.colostate.edu/Improve/wp-content/uploads/2016/04/UCDStatus0906_McDade.pdf)

McDade, C. (2007), Diminished wintertime nitrate concentrations in late 1990s, *IMPROVE Data Advisory 0002*. [http://vista.cira.colostate.edu/improve/Data/QA\\_QC/Advisory/da0002/da0002\\_WinterNO3.pdf](http://vista.cira.colostate.edu/improve/Data/QA_QC/Advisory/da0002/da0002_WinterNO3.pdf)

McDade, C. E., A. M. Dillner, and H. Indresand (2009), Particulate matter sample deposit geometry and effective filter face velocities, *Journal of the Air & Waste Management Association*, 59(9), 1045-1048, doi:DOI:10.3155/1047-3289.59.9.1045.

Pitchford, M. L., and W. C. Malm (1994), Development and applications of a standard visual index, *Atmospheric Environment*, 28(5), 1049-1054, doi:[https://doi.org/10.1016/1352-2310\(94\)90264-X](https://doi.org/10.1016/1352-2310(94)90264-X).

Pitchford, M., W. C. Malm, B. A. Schichtel, N. Kumar, D. Lowenthal, and J. L. Hand (2007), Revised algorithm for estimating light extinction from IMPROVE particle speciation data, *Journal of the Air & Waste Management Association*, 57(11), 1326-1336, doi:doi:10.3155/1047-3289.57.11.1326.

Schichtel, B. A. (2003), Underestimation of Sulfur Concentrations During High Loadings and Humidity Conditions in the Eastern US, *IMPROVE Data Advisory 0001*. [http://vista.cira.colostate.edu/improve/Data/QA\\_QC/Advisory/da0001/da0001\\_S\\_underestimation.htm](http://vista.cira.colostate.edu/improve/Data/QA_QC/Advisory/da0001/da0001_S_underestimation.htm)

Schichtel, B. A., W. C. Malm, M. Beaver, S. Copeland, J. L. Hand, A. J. Prenni, J. Rice, and J. Vimont (2021), The Future of Carbonaceous Aerosol Measurement in the IMPROVE Monitoring Program, [http://vista.cira.colostate.edu/improve/wp-content/uploads/2021/10/041\\_CarbonReport\\_Final.pdf](http://vista.cira.colostate.edu/improve/wp-content/uploads/2021/10/041_CarbonReport_Final.pdf)

Spada, N. J., S. Yatkin, J. Giacomo, K. Trzepla, and N. P. Hyslop (2023), Evaluating IMPROVE PM2.5 element measurements, *Journal of the Air & Waste Management Association*, 1-10, doi:10.1080/10962247.2023.2262417.

White, W. H. (2006), Elemental concentrations above the MDL can go undetected, *IMPROVE Data Advisory 0010*. [http://vista.cira.colostate.edu/improve/Data/QA\\_QC/Advisory/da0010/da0010\\_Almdl.pdf](http://vista.cira.colostate.edu/improve/Data/QA_QC/Advisory/da0010/da0010_Almdl.pdf)

White, W. H. (2007a), Varying bias of XRF sulfur relative to IC sulfate, *IMPROVE Data Advisory* 0012,  
[http://vista.cira.colostate.edu/improve/Data/QA\\_QC/Advisory/da0012/da0012\\_SSO4.pdf](http://vista.cira.colostate.edu/improve/Data/QA_QC/Advisory/da0012/da0012_SSO4.pdf).

White, W. H. (2007b), Shift in EC/OC split with 1 January 2005 TOR hardware upgrade, *IMPROVE Data Advisory* 0016,  
[http://vista.cira.colostate.edu/improve/Data/QA\\_QC/Advisory/da0016/da0016\\_TOR2005.pdf](http://vista.cira.colostate.edu/improve/Data/QA_QC/Advisory/da0016/da0016_TOR2005.pdf).

White, W. H. (2009), Inconstant bias in XRF sulfur - Advisory Update to da0012, *IMPROVE Data Advisory* 0023,  
[http://vista.cira.colostate.edu/improve/Data/QA\\_QC/Advisory/da0023/da0023\\_DA\\_SSO4\\_update.pdf](http://vista.cira.colostate.edu/improve/Data/QA_QC/Advisory/da0023/da0023_DA_SSO4_update.pdf)

White, W. H. (2015), Changed reporting of light absorption, *IMPROVE Data Advisory* 0033,  
[http://vista.cira.colostate.edu/improve/Data/QA\\_QC/Advisory/da0033/da0033\\_Fabs.pdf](http://vista.cira.colostate.edu/improve/Data/QA_QC/Advisory/da0033/da0033_Fabs.pdf)

White, W. H. (2016), Increased variation of humidity in the weighing laboratory, *IMPROVE Data Advisory* 0035,  
[http://vista.cira.colostate.edu/improve/Data/QA\\_QC/Advisory/da0035/da0035\\_IncreasedRH.pdf](http://vista.cira.colostate.edu/improve/Data/QA_QC/Advisory/da0035/da0035_IncreasedRH.pdf).

White, W. H., K. Trzepla, N. P. Hyslop, and B. A. Schichtel (2016), A critical review of filter transmittance measurements for aerosol light absorption, and de novo calibration for a decade of monitoring on PTFE membranes, *Aerosol Science and Technology*, 50(9), 984-1002, doi:<http://dx.doi.org/10.1080/02786826.2016.1211615>.

Zhang, X. (2019), Correction of chloride concentrations for filter blank levels, *IMPROVE Data Advisory* 0039,  
[http://vista.cira.colostate.edu/improve/Data/QA\\_QC/Advisory/da0039/da0039\\_ChlorideOverCorrection.pdf](http://vista.cira.colostate.edu/improve/Data/QA_QC/Advisory/da0039/da0039_ChlorideOverCorrection.pdf).

## Appendix A. Site Locations

**Table A1. Currently operating and discontinued IMPROVE particulate monitoring sites. Sites are grouped by region, as displayed in Figure 1.**

Site Name	Site Code	State	Latitude	Longitude	Elevation (m)	Dates of Operation
<b>Alaska</b>						
Ambler	AMBL1	AK	67.099	-157.863	77	09/03/2003-11/29/2004
Denali NP	DENA1	AK	63.723	-148.968	658	03/02/1988-present
Gates of the Arctic NP	GAAR1	AK	66.903	-151.517	196	11/02/2008-10/30/2015
Kenai Peninsula Borough	KPBO1	AK	60.012	-151.711	5	08/19/2015-present
Petersburg	PETE1	AK	56.611	-132.812	0	07/02/2004-09/28/2009
Simeonof	SIME1	AK	55.325	-160.506	57	09/13/2001-present
Toolik Lake Field Station	TOOL1	AK	68.632	-149.606	740	11/01/2018-present
Trapper Creek	TRCR1	AK	62.315	-150.316	155	09/13/2001-present
Tuxedni	TUXE1	AK	59.992	-152.666	15	12/03/2001-01/12/2015
<b>Alberta</b>						
Barrier Lake	BALA1	AB	51.029	-115.034	1391	01/15/2011-03/29/2017
<b>Appalachia</b>						
Arendtsville	AREN1	PA	39.923	-77.308	267	04/04/2001-12/31/2010
Cohutta	COHU1	GA	34.785	-84.626	735	06/03/2000-present
Dolly Sods WA	DOSO1	WV	39.105	-79.426	1182	09/04/1991-present
Frostburg Reservoir	FRRE1	MD	39.706	-79.012	767	03/01/2004-present
Great Smoky Mountains NP	GRSM1	TN	35.633	-83.942	810	03/02/1988-present
James River Face WA	JARI1	VA	37.627	-79.513	290	06/03/2000-present
Jefferson NF	JEFF1	VA	37.617	-79.483	219	09/1994-02/26/2000
Linville Gorge WA	LIGO1	NC	35.972	-81.933	969	04/01/2000-present
Shenandoah NP	SHEN1	VA	38.523	-78.435	1079	03/02/1988-present
Shining Rock WA	SHRO1	NC	35.394	-82.774	1617	06/01/1994-present
Sipsey WA	SIPS1	AL	34.343	-87.339	286	03/04/1992-present
<b>Boundary Waters</b>						
Boundary Waters Canoe Area WA	BOWA1	MN	47.947	-91.496	527	06/01/1991-present
Forest County Potawatomi Community	FCPC1	WI	45.565	-88.808	564	11/17/2016-present
Isle Royale NP	ISLE1	MI	47.46	-88.149	182	11/17/1999-present
Isle Royale NP	ISRO1	MI	47.917	-89.15	213	06/01/1988-12/29/1999
Seney	SENE1	MI	46.289	-85.95	215	11/17/1999-present
Voyageurs NP #1	VOYA1	MN	48.413	-92.83	426	03/02/1988-12/29/1999
Voyageurs NP #2	VOYA2	MN	48.413	-92.829	429	03/02/1999-present
<b>California Coast</b>						
Pinnacles NP	PINN1	CA	36.483	-121.157	302	03/02/1988-present
Point Reyes NS	PORE1	CA	38.122	-122.909	97	03/02/1988-present
San Rafael WA	RAFA1	CA	34.734	-120.007	956	02/02/2000-present
<b>Central Great Plains</b>						
Blue Mounds	BLMO1	MN	43.716	-96.191	473	06/01/2002-12/29/2015
Bondville	BOND1	IL	40.052	-88.373	263	03/08/2001-present
Cedar Bluff	CEBL1	KS	38.77	-99.763	666	06/01/2002-present

Site Name	Site Code	State	Latitude	Longitude	Elevation (m)	Dates of Operation
Crescent Lake	CRES1	NE	41.763	-102.434	1207	06/01/2002-12/29/2015
El Dorado Springs	ELDO1	MO	37.701	-94.035	298	03/03/2002-12/29/2015
Great River Bluffs	GRRI1	MN	43.937	-91.405	370	06/01/2002-present
Lake Sugema #1	LASU1	IA	40.688	-91.988	210	05/08/2002-11/29/2004
Lake Sugema #2	LASU2	IA	40.693	-92.006	229	12/02/2004-present
Nebraska NF	NEBR1	NE	41.889	-100.339	883	06/01/2002-present
Omaha	OMAH1	NE	42.149	-96.432	430	06/02/2003-08/04/2008
Sac and Fox	SAFO1	KS	39.979	-95.568	293	06/01/2002-06/29/2011
Tallgrass	TALL1	KS	38.434	-96.56	390	09/02/2002-present
Viking Lake	VILA1	IA	40.969	-95.045	371	05/08/2002-present
<b>Central Rocky Mountains</b>						
Brooklyn Lake	BRLA1	WY	41.366	-106.242	3196	07/31/1993-01/31/2004
Dinosaur NM	DINO1	CO	40.25	-108.967	1829	11/01/2018-present
Fort Collins	FOCO1	CO	40.593	-105.143	1572	07/2020-present
Fort Collins	FOCO2	CO	40.593	-105.143	1572	07/2020-present
Flat Tops	FLTO1	CO	39.915	-107.635	2593	10/27/2011-09/28/2021
Great Sand Dunes NP	GRSA1	CO	37.725	-105.519	2498	03/02/1988-present
Mount Zirkel WA	MOZI1	CO	40.538	-106.677	3243	06/01/1994-present
Ripple Creek	RICR1	CO	40.087	-107.314	2934	03/02/2009-10/30/2011
Rocky Mountain NP Headquarters	RMHQ1	CO	40.362	-105.564	2408	03/02/1988-12/29/1999
Rocky Mountain NP	ROMO1	CO	40.278	-105.546	2760	09/01/1990-present
Storm Peak	STPE1	CO	40.445	-106.74	3220	12/01/1993-12/29/1999
Shamrock Mine	SHMI1	CO	37.304	-107.484	2351	08/01/2004-12/27/2021
Wheeler Peak	WHPE1	NM	36.585	-105.452	3366	08/16/2000-present
White River NF	WHRI1	CO	39.154	-106.821	3414	06/02/1993-present
<b>Colorado Plateau</b>						
Arches NP	ARCH1	UT	38.783	-109.583	1722	03/02/1988-12/29/1999
Bandelier NM	BAND1	NM	35.78	-106.266	1988	03/02/1988-present
Bryce Canyon NP	BRCA1	UT	37.618	-112.174	2481	03/02/1988-present
Canyonlands NP	CANY1	UT	38.459	-109.821	1798	03/02/1988-present
Capitol Reef NP	CAPI1	UT	38.302	-111.293	1896	04/19/2000-present
Hopi Point	GRCA1	AZ	36.066	-112.154	2164	03/02/1988-12/29/1999
Hance Camp at Grand Canyon NP	GRCA2	AZ	35.973	-111.984	2267	03/02/1996-present
Indian Gardens	INGA1	AZ	36.078	-112.129	1166	09/02/1989-05/13/2013
Meadview	MEAD1	AZ	36.019	-114.068	902	09/04/1991-02/27/2021
Mesa Verde NP	MEVE1	CO	37.198	-108.491	2172	03/02/1988-present
San Pedro Parks WA	SAPE1	NM	36.014	-106.845	2935	08/16/2000-present
Weminuche WA	WEMI1	CO	37.659	-107.8	2750	03/02/1988-present
Zion Canyon	ZICA1	UT	37.198	-113.151	1215	12/01/2002-present
Zion NP	ZION1	UT	37.459	-113.224	1545	03/25/2000-08/22/2004
<b>Columbia River Gorge</b>						
Columbia Gorge	COGO1	WA	45.569	-122.21	230	09/18/1996-10/30/2011
Columbia River Gorge	CORI1	WA	45.664	-121.001	178	06/02/1993-present
<b>Death Valley</b>						
Death Valley NP	DEVA1	CA	36.509	-116.848	130	09/04/1993-04/28/2013
<b>East Coast</b>						
Brigantine NWR	BRIG1	NJ	39.465	-74.449	5	09/04/1991-present
Swanquarter	SWAN1	NC	35.451	-76.208	-4	06/10/2000-present

Site Name	Site Code	State	Latitude	Longitude	Elevation (m)	Dates of Operation
<b>Great Basin</b>						
Great Basin NP	GRBA1	NV	39.005	-114.216	2066	03/04/1992-present
Jarbridge WA	JARB1	NV	41.893	-115.426	1869	03/02/1988-present
<b>Hawaii</b>						
Haleakala Crater	HACR1	HI	20.759	-156.248	2158	01/24/2007-present
Haleakala NP	HALE1	HI	20.809	-156.282	1153	12/01/1990-05/30/2012
Hawaii Volcanoes NP	HAVO1	HI	19.431	-155.258	1259	03/02/1988-present
Mauna Loa Observatory #1	MALO1	HI	19.536	-155.577	3439	12/02/1992-08/28/2004
Mauna Loa Observatory #2	MALO2	HI	19.536	-155.577	3439	12/02/1992-08/28/2004
Mauna Loa Observatory #3	MALO3	HI	19.539	-155.578	3400	03/06/1996-02/26/2000
Mauna Loa Observatory #4	MALO4	HI	19.539	-155.578	3400	03/02/1996-02/26/2000
<b>Hells Canyon</b>						
Craters of the Moon NM	CRMO1	ID	43.461	-113.555	1818	03/04/1992-present
Hells Canyon	HECA1	OR	44.97	-116.844	655	09/03/2000-present
Sawtooth NF	SAWT1	ID	44.171	-114.927	1990	12/01/1993-present
Scoville	SCOV1	ID	43.65	-113.033	1500	03/04/1992-02/26/2000
Starkey	STAR1	OR	45.225	-118.513	1259	03/15/2000-present
<b>Korea</b>						
Baengnyeong Island	BYIS1		37.966	124.631	100	03/20/2013-present
<b>Lone Peak</b>						
Lone Peak WA	LOPE1	UT	40.445	-111.708	1768	12/01/1993-08/29/2001
<b>Mid South</b>						
Caney Creek	CACR1	AR	34.454	-94.143	683	06/24/2000-present
Cherokee Nation	CHER1	OK	36.956	-97.031	342	09/02/2002-04/20/2010
Ellis	ELLI1	OK	36.085	-99.935	697	03/02/2002-10/18/2015
Hercules-Glades	HEGL1	MO	36.614	-92.922	404	03/02/2001-present
Sikes	SIKE1	LA	32.057	-92.435	45	03/02/2001-12/31/2010
Southern Great Plains	SOGP1	OK	36.605	-97.485	315	10/01/2019-present
Stilwell	STIL1	OK	35.75	-94.67	300	04/23/2010-present
Upper Buffalo WA	UPBU1	AR	35.826	-93.203	723	12/24/1991-present
Wichita Mountains	WIMO1	OK	34.732	-98.713	509	03/02/2001-present
<b>Mogollon Plateau</b>						
Mount Baldy	BALD1	AZ	34.058	-109.441	2509	03/01/2000-present
Bosque del Apache	BOAP1	NM	33.87	-106.852	1390	04/15/2000-present
Gila WA	GICL1	NM	33.22	-108.235	1776	03/02/1994-present
Hillside	HILL1	AZ	34.429	-112.963	1511	04/19/2001-05/31/2005
Ike's Backbone	IKBA1	AZ	34.341	-111.683	1298	03/29/2000-present
Petrified Forest NP	PEFO1	AZ	35.078	-109.769	1766	03/02/1988-present
San Andres	SAAN1	NM	32.687	-106.484	1326	07/30/1997-02/26/2000
Sierra Ancha	SIAN1	AZ	34.091	-110.942	1600	02/09/2000-12/03/2017
Sycamore Canyon #1	SYCA1	AZ	35.141	-111.969	2046	09/04/1991-10/30/2015
Sycamore Canyon #2	SYCA2	AZ	35.164	-111.982	2046	10/24/2015-present
Tonto	TONT1	AZ	33.655	-111.107	775	03/02/1988-present
White Mountain	WHIT1	NM	33.469	-105.535	2064	12/03/2001-present
<b>Northeast</b>						

Site Name	Site Code	State	Latitude	Longitude	Elevation (m)	Dates of Operation
Acadia NP	ACAD1	ME	44.377	-68.261	157	03/02/1988-present
Addison Pinnacle	ADPI1	NY	42.091	-77.21	512	04/04/2001-06/28/2010
Bridgton	BRMA1	ME	44.107	-70.729	234	03/14/2001-12/29/2015
Casco Bay	CABA1	ME	43.833	-70.064	27	03/14/2001-present
Cape Cod	CACO1	MA	41.976	-70.024	49	04/04/2001-present
Connecticut Hill	COHI1	NY	42.401	-76.653	519	04/04/2001-06/25/2006
Great Gulf WA	GRGU1	NH	44.308	-71.218	454	06/03/1995-present
Londonderry	LOND1	NH	42.862	-71.380	124	01/03/2011-present
Lye Brook WA	LYBR1	VT	43.148	-73.127	1015	09/04/1991-09/30/2012
Lye Brook WA	LYEB1	VT	42.956	-72.91	882	01/01/2012-present
Martha's Vineyard	MAVI1	MA	41.331	-70.785	3	12/01/2002-present
Mohawk Mt.	MOMO1	CT	41.821	-73.297	522	09/13/2001-present
Moosehorn NWR	MOOS1	ME	45.126	-67.266	78	12/03/1994-present
Old Town	OLTO1	ME	44.933	-68.646	51	06/27/2001-05/29/2006
Pack Monadnock Summit	PACK1	NH	42.862	-71.879	695	10/03/2007-present
Penobscot	PENO1	ME	44.948	-68.648	45	01/11/2006-present
Proctor Maple Research Facility	PMRF1	VT	44.528	-72.869	401	12/01/1993-present
Presque Isle	PRIS1	ME	46.696	-68.033	166	03/08/2001-present
Quabbin Summit	QURE1	MA	42.298	-72.335	318	04/04/2001-12/29/2015
<b>Northern Great Plains</b>						
Badlands NP	BADL1	SD	43.743	-101.941	736	03/02/1988-present
Cloud Peak	CLPE1	WY	44.334	-106.957	2471	06/01/2002-07/29/2015
Fort Peck	FOPE1	MT	48.308	-105.102	638	06/01/2002-present
Lostwood	LOST1	ND	48.642	-102.402	696	12/15/1999-present
Medicine Lake	MELA1	MT	48.487	-104.476	606	12/15/1999-present
Northern Cheyenne	NOCH1	MT	45.65	-106.557	1283	06/01/2002-present
Thunder Basin	THBA1	WY	44.663	-105.287	1195	06/01/2002-12/29/2019
Theodore Roosevelt NP	THRO1	ND	46.895	-103.378	853	12/15/1999-present
UL Bend	ULBE1	MT	47.582	-108.72	891	01/26/2000-present
Wind Cave NP	WICA1	SD	43.558	-103.484	1296	12/15/1999-present
<b>Northern Rocky Mountains</b>						
Boulder Lake	BOLA1	WY	42.846	-109.640	2296	08/26/2009-present
Bridger WA	BRID1	WY	42.975	-109.758	2627	03/02/1988-present
Cabinet Mountains	CABI1	MT	47.955	-115.671	1441	07/26/2000-present
Flathead	FLAT1	MT	47.773	-114.269	1580	06/01/2002-present
Gates of the Mountains	GAMO1	MT	46.826	-111.711	2387	07/26/2000-present
Glacier NP	GLAC1	MT	48.511	-113.997	975	03/02/1988-present
Monture	MONT1	MT	47.122	-113.154	1282	03/29/2000-present
North Absaroka	NOAB1	WY	44.745	-109.382	2482	01/26/2000-present
Salmon NF	SALM1	ID	45.159	-114.026	2788	12/01/1993-11/05/2000
Sula Peak	SULA1	MT	45.86	-114	1896	06/01/1994-present
Yellowstone NP #1	YELL1	WY	44.565	-110.4	2442	03/09/1988-12/29/1999
Yellowstone NP #2	YELL2	WY	44.565	-110.4	2425	03/02/1988-present
<b>Northwest</b>						
Lynden	LYND1	WA	48.953	-122.559	28	10/16/1996-12/29/1999
Makah Indian Reservation #1	MAKA1	WA	48.372	-124.595	9	09/02/2006-10/29/2010

Site Name	Site Code	State	Latitude	Longitude	Elevation (m)	Dates of Operation
Makah Indian Reservation #2	MAKA2	WA	48.298	-124.625	480	11/01/2010-present
Mount Rainier NP	MORA1	WA	46.758	-122.124	439	03/02/1988-present
North Cascades	NOCA1	WA	48.732	-121.065	568	07/30/1997-present
Olympic NP	OLYM1	WA	48.007	-122.973	599	07/12/2001-present
Pasayten	PASA1	WA	48.388	-119.928	1627	11/02/2000-present
Snoqualmie Pass	SNPA1	WA	47.422	-121.426	1049	06/02/1993-present
Spokane Reservation	SPOK1	WA	47.905	-117.861	552	07/12/2001-06/30/2005
White Pass	WHPA1	WA	46.624	-121.388	1827	02/16/2000-present
<b>Not Assigned</b>						
Walker River Paiute Tribe	WARI1	NV	38.952	-118.815	1250	06/02/2003-10/31/2005
<b>Ohio River Valley</b>						
Cadiz	CADI1	KY	36.784	-87.85	192	03/08/2001-12/31/2010
Livonia	LIVO1	IN	38.535	-86.26	281	03/08/2001-12/31/2010
Mammoth Cave NP	MACA1	KY	37.132	-86.148	235	09/04/1991-present
Mingo	MING1	MO	36.972	-90.143	111	06/03/2000-present
M.K. Goddard	MKGO1	PA	41.427	-80.145	380	04/04/2001-12/31/2010
Quaker City	QUCI1	OH	39.943	-81.338	366	04/04/2001-present
<b>Ontario</b>						
Egbert	EGBE1	ON	44.231	-79.783	251	9/01/2005-present
<b>Oregon and Northern California</b>						
Bliss SP	BLIS1	CA	38.976	-120.103	2131	09/01/1990-present
Crater Lake NP	CRLA1	OR	42.896	-122.136	1996	03/02/1988-present
Kalmiopsis	KALM1	OR	42.552	-124.059	80	03/11/2000-present
Lava Beds NM	LABE1	CA	41.712	-121.507	1460	03/29/2000-present
Lassen Volcanic NP	LAVO1	CA	40.54	-121.577	1733	03/02/1988-present
Lake Tahoe Community College	LTCC1	CA	38.925	-119.98	1935	02/19/2014-present
Mount Hood	MOHO1	OR	45.289	-121.784	1531	03/15/2000-present
Redwood NP	REDW1	CA	41.561	-124.084	244	03/02/1988-present
Three Sisters WA	THSI1	OR	44.291	-122.043	885	06/02/1993-present
Trinity	TRIN1	CA	40.786	-122.805	1014	10/18/2000-present
<b>Phoenix</b>						
Phoenix	PHOE1	AZ	33.504	-112.096	342	04/19/2001-present
Phoenix	PHOE5	AZ	33.504	-112.096	342	01/01/2005-present
<b>Puget Sound</b>						
Puget Sound	PUSO1	WA	47.57	-122.312	98	03/02/1996-present
<b>Sierra Nevada</b>						
Dome Lands WA	DOLA1	CA	35.699	-118.202	914	06/01/1994-12/29/1999
Dome Lands WA	DOME1	CA	35.728	-118.138	927	02/02/2000-present
Hoover	HOOV1	CA	38.088	-119.177	2561	06/06/2001-present
Kaiser	KAIS1	CA	37.221	-119.155	2598	01/26/2000-present
Owens Valley	OWVL1	CA	37.361	-118.331	1234	06/27/2013-present
Sequoia NP	SEQU1	CA	36.489	-118.829	519	03/04/1992-present
South Lake Tahoe	SOLA1	CA	38.933	-119.967	1900	03/01/1989-12/29/1999
Yosemite NP	YOSE1	CA	37.713	-119.706	1603	03/02/1988-present
<b>Southeast</b>						
Breton	BRET1	LA	29.119	-89.207	11	08/16/2000-08/29/2005
Breton Island	BRIS1	LA	30.109	-89.762	-7	01/16/2008-present
Chassahowitzka NWR	CHAS1	FL	28.748	-82.555	4	03/03/1993-present

Site Name	Site Code	State	Latitude	Longitude	Elevation (m)	Dates of Operation
Everglades NP	EVER1	FL	25.391	-80.681	1	09/03/1988-present
Okefenokee NWR	OKEF1	GA	30.741	-82.128	48	09/04/1991-present
Cape Romain NWR	ROMA1	SC	32.941	-79.657	5	09/03/1994-present
St. Marks NWR	SAMA1	FL	30.093	-84.161	7	08/16/2000-present
<b>Southern Arizona</b>						
Chiricahua NM	CHIR1	AZ	32.009	-109.389	1555	03/02/1988-present
Douglas	DOUG1	AZ	31.349	-109.54	1230	06/02/2004-10/30/2015
Nogales	NOGA1	AZ	31.338	-110.937	1172	10/27/2015-present
Organ Pipe	ORPI1	AZ	31.951	-112.802	504	12/01/2002-present
Queen Valley	QUVA1	AZ	33.294	-111.286	661	04/19/2001-12/29/2015
Saguaro NP	SAGU1	AZ	32.175	-110.737	941	06/01/1988-present
Saguaro West	SAWE1	AZ	32.249	-111.218	714	10/31/2001-present
<b>Southern California</b>						
Agua Tibia	AGTI1	CA	33.464	-116.971	508	12/20/2000-present
Joshua Tree NP	JOSH1	CA	34.069	-116.389	1235	02/23/2000-present
Joshua Tree NP	JOTR1	CA	34.069	-116.389	1228	09/04/1991-12/29/1999
San Gabriel	SAGA1	CA	34.297	-118.028	1791	12/03/2001-present
San Gorgonio WA	SAGO1	CA	34.194	-116.913	1726	03/02/1988-present
Wrightwood	WRIG1	CA	34.38	-117.69	2106	10/01/2009-10/15/2012
<b>Urban Quality Assurance Sites</b>						
Atlanta	ATLA1	GA	33.688	-84.29	243	03/01/2004-present
Baltimore	BALT1	MD	39.255	-76.709	78	06/02/2004-12/31/2006
Birmingham	BIRM1	AL	33.553	-86.815	176	03/01/2004-present
Chicago	CHIC1	IL	41.751	-87.713	195	09/03/2003-08/29/2005
Detroit	DETR1	MI	42.229	-83.209	180	09/03/2003-present
Fresno	FRES1	CA	36.782	-119.773	100	09/03/2004-present
Houston	HOUS1	TX	29.67	-95.129	7	03/01/2004-08/29/2005
New York City	NEYO1	NY	40.816	-73.902	45	08/01/2004-06/07/2010
Pittsburgh	PITT1	PA	40.465	-79.961	268	03/01/2004-present
Rubidoux	RUBI1	CA	34.0	-117.416	248	09/03/2004-08/29/2005
<b>Virgin Islands</b>						
Virgin Islands NP	VIIS1	VI	18.336	-64.796	51	09/01/1990-present
<b>Washington D.C.</b>						
Washington D.C.	WASH1	DC	38.876	-77.034	15	03/02/1988-06/08/2015
<b>West Texas</b>						
Big Bend NP	BIBE1	TX	29.303	-103.178	1067	03/02/1988-present
Carlsbad Caverns NP	CAVE1	NM	32.178	-104.444	1355	07/30/2017-present
Guadalupe Mountains NP	GUMO1	TX	31.833	-104.809	1672	03/02/1988-present
Salt Creek	SACR1	NM	33.46	-104.404	1072	04/08/2000-present

## Appendix B. Tables from the Federal Land Manager Environmental Database

**Table B1. Description of available IMPROVE data.**

IMPROVE Dataset	Frequency	Description
IMPROVE Aerosol	1-in-3 day	Site-specific 24-hr validated and blank-corrected mass data for all available parameters.
IMPROVE Aerosol Preliminary	1-in-3 day	Site-specific 24-hr preliminary mass data. These data are made available as quickly as possible. No validations have been performed, blank corrections are estimated, minimum detection limits (MDL) and uncertainties are unavailable. Status flags may include internal values not delivered with final data. These data should not be used for official analyses or investigations (Level 0 data).
IMPROVE Natural Conditions (2064)	Once	Site-specific Regional Haze Rule (RHR) natural conditions mass and aerosol extinction values for the year 2064.
IMPROVE Nephelometer	Hourly	Site-specific nephelometer-measured ambient light scattering coefficients, internal instrument temperature, ambient temperature and station relative humidity.
IMPROVE RHR2 5yr Avg	Annual	Site-specific RHR2 (haziest conditions metric) five year reconstructed mass and light extinction values for 10 <sup>th</sup> , 50 <sup>th</sup> , 90 <sup>th</sup> percentiles and group 100 (annual average).
IMPROVE RHR2 Group Means	Annual	Site-specific RHR2 (haziest conditions metric) annual reconstructed mass and light extinction values for 10 <sup>th</sup> , 50 <sup>th</sup> , 90 <sup>th</sup> percentiles and group 100 (annual average).
IMPROVE RHR2 Metrics	1-in-3 day	Site-specific 24-hr RHR2 (haziest conditions metric) reconstructed mass and light extinction values and corresponding percentile groups.
IMPROVE RHR3 5yr Avg	Annual	Site-specific RHR3 (impairment metric) five year reconstructed mass and light extinction values for 10 <sup>th</sup> , 50 <sup>th</sup> , 90 <sup>th</sup> percentiles and group 100 (annual average).
IMPROVE RHR3 Endpoints (2064)	Once	Site-specific 2064 endpoint values for reconstructed mass and light extinction coefficients for RHR3 (impairment) metric.
IMPROVE RHR3 Group Means	Annual	Site-specific RHR3 (impairment metric) annual reconstructed mass and light extinction values for 10 <sup>th</sup> , 50 <sup>th</sup> , 90 <sup>th</sup> percentiles and group 100 (annual average).
IMPROVE RHR3 Metrics	1-in-3 day	Site-specific 24-hr RHR3 (impairment metric) reconstructed mass and light extinction values and corresponding percentile groups.

**Table B2. Parameters available for download in FED. The “f” in the parameter code name refers to the “fine” PM<sub>2.5</sub> size range. Parameters are organized by analysis or measurement type.**

Parameter Code	Parameter Name	Units	EPA Code	Description
Elements (X-Ray Fluorescence, XRF)				
Alf	Aluminum (Fine)	$\mu\text{g m}^{-3}$	88104	

Parameter Code	Parameter Name	Units	EPA Code	Description
ASf	Arsenic (Fine)	$\mu\text{g m}^{-3}$	88103	
BRf	Bromine (Fine)	$\mu\text{g m}^{-3}$	88109	
CAF	Calcium (Fine)	$\mu\text{g m}^{-3}$	88111	
CLf	Chlorine (Fine)	$\mu\text{g m}^{-3}$	88115	
CRf	Chromium (Fine)	$\mu\text{g m}^{-3}$	88112	
CUf	Copper (Fine)	$\mu\text{g m}^{-3}$	88114	
FEf	Iron (Fine)	$\mu\text{g m}^{-3}$	88126	
PBf	Lead (Fine)	$\mu\text{g m}^{-3}$	88128	
MGf	Magnesium (Fine)	$\mu\text{g m}^{-3}$	88140	
MNf	Manganese (Fine)	$\mu\text{g m}^{-3}$	88132	
NIf	Nickel (Fine)	$\mu\text{g m}^{-3}$	88136	
Pf	Phosphorus (Fine)	$\mu\text{g m}^{-3}$	88152	
Kf	Potassium (Fine)	$\mu\text{g m}^{-3}$	88180	
RBf	Rubidium (Fine)	$\mu\text{g m}^{-3}$	88176	
SEf	Selenium (Fine)	$\mu\text{g m}^{-3}$	88154	
SIf	Silicon (Fine)	$\mu\text{g m}^{-3}$	88165	
NAf	Sodium (Fine)	$\mu\text{g m}^{-3}$	88184	
SRf	Strontium (Fine)	$\mu\text{g m}^{-3}$	88168	
Sf	Sulfur (Fine)	$\mu\text{g m}^{-3}$	88169	
TIf	Titanium (Fine)	$\mu\text{g m}^{-3}$	88161	
Vf	Vanadium (Fine)	$\mu\text{g m}^{-3}$	88164	
ZNf	Zinc (Fine)	$\mu\text{g m}^{-3}$	88167	
ZRf	Zirconium (Fine)	$\mu\text{g m}^{-3}$	88185	
<b>Ions (Ion Chromatography)</b>				
CHLf	Chloride (Fine)	$\mu\text{g m}^{-3}$	88203	
NO3f	Nitrate (Fine)	$\mu\text{g m}^{-3}$	88306	
N2f	Nitrite (Fine)	$\mu\text{g m}^{-3}$	88338	
SO4f	Sulfate (Fine)	$\mu\text{g m}^{-3}$	88403	
<b>Carbon (Thermal Optical Reflectance and Transmittance, TOR or TOT, respectively)</b>				
OC1f	Carbon, Organic Fraction 1 (Fine)	$\mu\text{g m}^{-3}$	88324	TOR, pure helium (>99.999%) atmosphere, temperature (T) = 140 °C
OC2f	Carbon, Organic Fraction 2 (Fine)	$\mu\text{g m}^{-3}$	88325	TOR, pure helium (>99.999%) atmosphere, T = 280 °C
OC3f	Carbon, Organic Fraction 3 (Fine)	$\mu\text{g m}^{-3}$	88326	TOR, pure helium (>99.999%) atmosphere, T = 480 °C
OC4f	Carbon, Organic Fraction 4 (Fine)	$\mu\text{g m}^{-3}$	88327	TOR, pure helium (>99.999%) atmosphere, T = 580 °C
OPf	Carbon, Organic Pyrolyzed (Fine), by Reflectance	$\mu\text{g m}^{-3}$	88328	TOR, carbon that is measured after the introduction of helium/oxygen atmosphere at 550 °C but before reflectance returns to initial value.
OPTf	Carbon, Organic Pyrolyzed (Fine), by Transmittance	$\mu\text{g m}^{-3}$	88336	TOT, carbon that is measured after the introduction of helium/oxygen

Parameter Code	Parameter Name	Units	EPA Code	Description
				atmosphere at 550 °C but before transmittance returns to initial value
OCf	Carbon, Organic Total (Fine)	$\mu\text{g m}^{-3}$	88320	Organic carbon from TOR carbon fractions (OC1f+OC2f+OC3f+OC4f+OPf)
EC1f	Carbon, Elemental Fraction 1 (Fine)	$\mu\text{g m}^{-3}$	88329	TOR, 98% helium, 2% oxygen atmosphere, temperature (T) = 580 °C.
EC2f	Carbon, Elemental Fraction 2 (Fine)	$\mu\text{g m}^{-3}$	88380	TOR, 98% helium, 2% oxygen atmosphere, T = 740 °C.
EC3f	Carbon, Elemental Fraction 3 (Fine)	$\mu\text{g m}^{-3}$	88331	TOR, 98% helium, 2% oxygen atmosphere, T = 840 °C.
ECf	Carbon, Elemental Total (Fine)	$\mu\text{g m}^{-3}$	88321	Elemental carbon from TOR carbon fractions (E1+E2+E3-OP)
RefF_405	Final laser reflectance at 405 nm	ratio		Final laser reflectance at 405 nm
RefF_445	Final laser reflectance at 445 nm	ratio		Final laser reflectance at 445 nm
RefF_532	Final laser reflectance at 532 nm	ratio		Final laser reflectance at 532 nm
RefF_635	Final laser reflectance at 635 nm	ratio		Final laser reflectance at 635 nm
RefF_780	Final laser reflectance at 780 nm	ratio		Final laser reflectance at 780 nm
RefF_808	Final laser reflectance at 808 nm	ratio		Final laser reflectance at 808 nm
RefF_980	Final laser reflectance at 980 nm	ratio		Final laser reflectance at 980 nm
TransF_405	Final laser transmittance at 405 nm	ratio		Final laser transmittance at 405 nm
TransF_445	Final laser transmittance at 445 nm	ratio		Final laser transmittance at 445 nm
TransF_532	Final laser transmittance at 532 nm	ratio		Final laser transmittance at 532 nm
TransF_635	Final laser transmittance at 635 nm	ratio		Final laser transmittance at 635 nm
TransF_780	Final laser transmittance at 780 nm	ratio		Final laser transmittance at 780 nm
TransF_808	Final laser transmittance at 808 nm	ratio		Final laser transmittance at 808 nm
TransF_980	Final laser transmittance at 980 nm	ratio		Final laser transmittance at 980 nm
RefI_405	Initial laser reflectance at 405 nm	ratio		Initial laser reflectance at 405 nm
RefI_445	Initial laser reflectance at 445 nm	ratio		Initial laser reflectance at 445 nm
RefI_532	Initial laser reflectance at 532 nm	ratio		Initial laser reflectance at 532 nm
RefI_635	Initial laser reflectance at 635 nm	ratio		Initial laser reflectance at 635 nm
RefI_780	Initial laser reflectance at 780 nm	ratio		Initial laser reflectance at 780 nm
RefI_808	Initial laser reflectance at 808 nm	ratio		Initial laser reflectance at 808 nm

Parameter Code	Parameter Name	Units	EPA Code	Description
RefI_980	Initial laser reflectance at 980 nm	ratio		Initial laser reflectance at 980 nm
TransI_405	Initial laser transmittance at 405 nm	ratio		Initial laser transmittance at 405 nm
TransI_445	Initial laser transmittance at 445 nm	ratio		Initial laser transmittance at 445 nm
TransI_532	Initial laser transmittance at 532 nm	ratio		Initial laser transmittance at 532 nm
TransI_635	Initial laser transmittance at 635 nm	ratio		Initial laser transmittance at 635 nm
TransI_780	Initial laser transmittance at 780 nm	ratio		Initial laser transmittance at 780 nm
TransI_808	Initial laser transmittance at 808 nm	ratio		Initial laser transmittance at 808 nm
TransI_980	Initial laser transmittance at 980 nm	ratio		Initial laser transmittance at 980 nm
RefM_405	Minimum laser reflectance at 405 nm	ratio		Minimum laser reflectance at 405 nm
RefM_445	Minimum laser reflectance at 445 nm	ratio		Minimum laser reflectance at 445 nm
RefM_532	Minimum laser reflectance at 532 nm	ratio		Minimum laser reflectance at 532 nm
RefM_635	Minimum laser reflectance at 635 nm	ratio		Minimum laser reflectance at 635 nm
RefM_780	Minimum laser reflectance at 780 nm	ratio		Minimum laser reflectance at 780 nm
RefM_808	Minimum laser reflectance at 808 nm	ratio		Minimum laser reflectance at 808 nm
RefM_980	Minimum laser reflectance at 980 nm	ratio		Minimum laser reflectance at 980 nm
TransM_405	Minimum laser transmittance at 405 nm	ratio		Minimum laser transmittance at 405 nm
TransM_445	Minimum laser transmittance at 445 nm	ratio		Minimum laser transmittance at 445 nm
TransM_532	Minimum laser transmittance at 532 nm	ratio		Minimum laser transmittance at 532 nm
TransM_635	Minimum laser transmittance at 635 nm	ratio		Minimum laser transmittance at 635 nm
TransM_780	Minimum laser transmittance at 780 nm	ratio		Minimum laser transmittance at 780 nm
TransM_808	Minimum laser transmittance at 808 nm	ratio		Minimum laser transmittance at 808 nm
TransM_980	Minimum laser transmittance at 980 nm	ratio		Minimum laser transmittance at 980 nm
OP405TR	Organic Pyrolyzed Carbon by Reflectance at 405 nm	$\mu\text{g m}^{-3}$		Organic Pyrolyzed Carbon by Reflectance at 405 nm
OP445TR	Organic Pyrolyzed Carbon by Reflectance at 445 nm	$\mu\text{g m}^{-3}$		Organic Pyrolyzed Carbon by Reflectance at 445 nm
OP532TR	Organic Pyrolyzed Carbon by Reflectance at 532 nm	$\mu\text{g m}^{-3}$		Organic Pyrolyzed Carbon by Reflectance at 532 nm
OP780TR	Organic Pyrolyzed Carbon by Reflectance at 780 nm	$\mu\text{g m}^{-3}$		Organic Pyrolyzed Carbon by Reflectance at 780 nm

Parameter Code	Parameter Name	Units	EPA Code	Description
OP808TR	Organic Pyrolyzed Carbon by Reflectance at 808 nm	$\mu\text{g m}^{-3}$		Organic Pyrolyzed Carbon by Reflectance at 808 nm
OP980TR	Organic Pyrolyzed Carbon by Reflectance at 980 nm	$\mu\text{g m}^{-3}$		Organic Pyrolyzed Carbon by Reflectance at 980 nm
OP405TT	Organic Pyrolyzed Carbon by Transmittance at 405 nm	$\mu\text{g m}^{-3}$		Organic Pyrolyzed Carbon by Transmittance at 405 nm
OP445TT	Organic Pyrolyzed Carbon by Transmittance at 445 nm	$\mu\text{g m}^{-3}$		Organic Pyrolyzed Carbon by Transmittance at 445 nm
OP532TT	Organic Pyrolyzed Carbon by Transmittance at 532 nm	$\mu\text{g m}^{-3}$		Organic Pyrolyzed Carbon by Transmittance at 532 nm
OP780TT	Organic Pyrolyzed Carbon by Transmittance at 780 nm	$\mu\text{g m}^{-3}$		Organic Pyrolyzed Carbon by Transmittance at 780 nm
OP808TT	Organic Pyrolyzed Carbon by Transmittance at 808 nm	$\mu\text{g m}^{-3}$		Organic Pyrolyzed Carbon by Transmittance at 808 nm
OP980TT	Organic Pyrolyzed Carbon by Transmittance at 980 nm	$\mu\text{g m}^{-3}$		Organic Pyrolyzed Carbon by Transmittance at 980 nm
<b>Other Measurements</b>				
fAbs	Filter Absorption Coefficient	$\text{Mm}^{-1}$	63102	A calibrated absorption coefficient measured from a Teflon filter using a hybrid integrating plate and sphere (HIPS) method
FlowRate	Flow Rate	LPM	68101	The rate of air flow through an air sampling instrument (Liter Per Minute)
MF	Mass, PM2.5 (Fine)	$\mu\text{g m}^{-3}$	88101	Gravimetric mass measurement for particles with aerodynamic diameters less than $2.5 \mu\text{m}$ .
MT	Mass, PM10 (Total)	$\mu\text{g m}^{-3}$	85101	Gravimetric mass measurement for particles with aerodynamic diameters less than $10 \mu\text{m}$ .
SampDur	Sampling Duration	minutes		The duration of a given sampling period in minutes
<b>Calculated Variables</b>				
ammNO3f	Ammonium Nitrate (Fine)	$\mu\text{g m}^{-3}$		$1.29 \times \text{NO3f}$
ammSO4f	Ammonium Sulfate (Fine)	$\mu\text{g m}^{-3}$		$1.375 \times \text{SO4f}$
OMCf	Carbon, Organic Mass (Fine) ( $1.8 \times \text{OC}$ )	$\mu\text{g m}^{-3}$		$1.8 \times \text{OCf}$
TCf	Carbon, Total (Fine)	$\mu\text{g m}^{-3}$		From TOR carbon fractions ( $\text{OCf} + \text{ECf}$ )
CM_calculated	Mass, PM10 – PM2.5 (Coarse)	$\mu\text{g m}^{-3}$		$\text{MT} - \text{MF}$
SeaSaltf	Sea Salt (Fine)	$\mu\text{g m}^{-3}$		$1.8 \times \text{CHLf}$
SOILf	Soil (Fine)	$\mu\text{g m}^{-3}$		$2.2 \times \text{ALf} + 2.49 \times \text{SIf} + 1.63 \times \text{CAF} + 2.42 \times \text{FEf} + 1.94 \times \text{TIf}$
RCFM	Mass, PM2.5 Reconstructed (Fine)	$\mu\text{g m}^{-3}$		Sum of ammSO4f, ammNO3f, OMCf, ECf, soilf, and seasaltf.
RCTM	Mass, PM10 Reconstructed (Total)	$\mu\text{g m}^{-3}$		Sum of ammSO4f, ammNO3f, OMCf, ECf, soilf, seasaltf, and CM calculated.

**Table B3. Field option choices for dataset download in FED.**

Field	Output Name	Description
Dataset	Dataset	The alphanumeric code used to identify the dataset.
Site	SiteCode	The alphanumeric code used to identify the site.
POC	POC	The "Parameter Occurrence Code" or sequence number. This number distinguishes samplers for sites with more than one sampler.
Date	Date	The date of the observation or measurement.
Parameter	ParamCode	The alphanumeric variable or parameter code.
Data Value	Val	The primary measurement or data value; A floating point number.
Method	Method	The method by which the value was measured or derived.
Unit	Unit	The units of measurement used when reporting the data value.
AuxID	AuxID	An auxiliary integer that can be used to further disambiguate the data value.
Status Flag	Status	The primary status code assigned to the data value during import.
Flag 1	ProviderFlag	Primary status flag assigned by the provider (UC Davis).
Flag 2	ObjectiveCode	Site Objective: RT = Routine, CL = Collocated
Flag 3	ModuleTypeCode	IMPROVE sampler taking the measurement (A, B, C, D)
Flag 4	POC	AQS Parameter Occurrence Code
Aux. Value 1	Unc	Measurement Uncertainty
Aux. Value 2	MDL	Minimum Detection Limit
Aux. Value 3	Val3	(not used)
Site Name	SiteName	The full name of the monitoring site
Latitude	Latitude	The latitude of the monitoring site in decimal degrees
Longitude	Longitude	The longitude of the monitoring site in decimal degrees
Elevation	Elevation	The elevation of the monitoring site in meters above mean sea level
State	State	The state or province where the site is located
County FIPS	CountyFIPS	The FIPS (Federal Information Processing Series) code of the county where the site is located
EPA Site Code	EPACode	The site code used by the EPA Air Quality System (AQS)

## Appendix C. Status Flags and Codes

**Table C1.** Status codes assigned during data import (noted as “Status Flag”) in Table B3.

Flag Code	Category	Description
H1	N/A	Historical data that have not been assessed or validated.
I0	Invalid	Invalid value - unknown reason
I1	Invalid	Invalid value - known reason
I2	Invalid	Invalid value (-999), though sample-level flag seems valid (SEM)
M1	Missing	Missing value because no value is available
M2	Missing	Missing value because invalidated by data originator
M3	Missing	Missing value due to clogged filter
NA	N/A	Not available from source data
V0	Valid	Valid value
V1	Valid	Valid value but comprised wholly or partially of below detection limit data
V2	Valid	Valid estimated value
V3	Valid	Valid interpolated value
V4	Valid	Valid value despite failing to meet some quality control or statistical criteria
V5	Valid	Valid value but qualified because of possible contamination
V6	Valid	Valid value but qualified due to non-standard sampling conditions
V7	Valid	Valid value set equal to the detection limit (DL) since the value was below the DL
VE	Valid	Valid value during air quality event
VM	Valid	Valid modeled value
VS	Valid	Valid substituted value

**Table C2.** Status flags and their definitions.

Status Flag	Description	Flag Type
BI	Bad Installation of Sample Cartridge or Filter	Terminal
CG	Sample Flow Rate Out of Spec.	Informational
CL	Sample Flow Rate Out of Limits	Terminal
DA	Sample not analyzed	Terminal
DE	Reported value is an estimate	Informational
EP	Equipment Problem	Terminal
LF	Sample Flow Rate Out of Spec.	Informational
NF	No Flow	Temporary
NM	Normal	Informational
NS	No Sample Collected/Late Sample Change	Terminal
OL	Site Off Line	Terminal
PO	Power Outage	Terminal
QD	Questionable Data	Temporary
SA	Sampling Anomaly	Informational
SO	Still out	Temporary
SP	Same-day Field Blank/Sample Swap	Informational
SW	Sampling Dates Swap	Informational
TO	Timing Outside normal bounds	Informational
TU	Incorrect Time (with time shift >= 6hrs)	Informational
UN	Undetermined Weight	Informational
XX	Sample Destroyed, Damaged or Contaminated	Terminal

PM	Undefined but allowed by SWAP as informational	No longer used
NR	Not Reanalyzed by DRI	No longer used
NA	Not Applicable	No longer used
QA	Quality Assurance	No longer used
QC	Quality Control	No longer used
RF	Really High Flow Rate	No longer used
PC	Possible Contamination	No longer used

**Table C3. Definitions and application criteria of automatic flow flags for PM<sub>2.5</sub> and PM<sub>10</sub>.**

Automatic Flow Flag	Definition	Type	Criteria for Application for PM <sub>2.5</sub> Samples	Criteria for Application for PM <sub>10</sub> Samples
CL	Clogged Filter	Terminal	Flow rate < 15 lpm for more than 6 hours if flashcard data are used Average flow rate < 15 lpm if log sheet values are used	Flow rate < 10 lpm for more than 6 hours if flashcard data are used Average flow rate < 10 lpm if log sheet values are used
CG	Clogging Filter	Informational	Flow rate < 18 lpm for more than 6 hours if flashcard data used Average flow rate < 18 lpm if log sheet values are used	Flow rate < 14 lpm for more than 6 hours if flashcard data are used; Average flow rate < 14 lpm if log sheet values are used
LF	Low/high flow rate	Informational	Average flow rate < 19.7 lpm or > 24.1 lpm	Average flow rate < 15 lpm or > 18 lpm
PO	Power Outage	Terminal	Elapsed time < 1080 minutes (18 hrs)	Elapsed time < 1080 minutes (18 hrs)
EP	Equipment Problem	Terminal	Elapsed time > 1800 minutes (30 hrs) or is missing	Elapsed time > 1800 minutes (30 hrs) or is missing
TO	Timing Outside normal bounds	Informational	Elapsed time between 1080 minutes (18 hrs) - 1380 minutes (23 hrs) or 1500 minutes (25 hrs) – 1800 minutes (30 hrs)	Elapsed time between 1080 minutes (18 hrs) - 1380 minutes (23 hrs) or 1500 minutes (25 hrs) – 1800 minutes (30 hrs)
SD	Short-duration sample	Terminal for RHR, but reported	Elapsed time < 18 hours and flow shutoff intentionally by software	Elapsed time < 18 hours and flow shutoff intentionally by software

## Appendix D. Uncertainty Estimates

Below is a discussion of uncertainty estimates taken from the IMPROVE SOP; see the IMPROVE [SOP](#) for more details.

### *PM<sub>2.5</sub> and PM<sub>10</sub> Mass (A and D modules)*

PM<sub>2.5</sub> mass is measured gravimetrically on the Teflon filter from the A module. PM<sub>10</sub> mass is measured gravimetrically on the Teflon filter from the D module. The pre- and post-weights ( $\mu\text{g filter}^{-1}$ ) are the mass of the filter before and after sampling, respectively. The mass concentration ( $C_{\text{Mass}}$ ), uncertainty ( $\sigma_{\text{Mass}}$ ), and MDL ( $\text{mdl}_{\text{Mass}}$ ) are calculated using the following equations and are in units of  $\mu\text{g m}^{-3}$ :

$$C_{\text{Mass}} = \left( \frac{\text{Postweight} - \text{preweight}}{V} \right) \quad (\text{D1})$$

$$\sigma_{\text{Mass}} = \frac{\sqrt{(0.608 \times \text{Max}(P95, \text{mdl}_{\text{analytical}}))^2 + (f \times (\text{postweight} - \text{preweight}))^2}}{V} \quad (\text{D2})$$

$$\text{mdl}_{\text{Mass}} = \frac{\text{Max}(P95, \text{mdl}_{\text{analytical}})}{V} \quad (\text{D3})$$

$V$  is the sample air volume ( $\text{m}^3$ ) and P95 is the 95<sup>th</sup> percentile of field blank measurements in  $\mu\text{g filter}^{-1}$ . The analytical MDL ( $\text{mdl}_{\text{analytical}}$ ) is reported from the analytical laboratory ( $10 \mu\text{g filter}^{-1}$  for PM<sub>2.5</sub> and PM<sub>10</sub>). The analytical MDL is considered the ‘floor value’ and is used as the reported MDL in the event that the median value of the field blanks is lower than the respective analytical MDL. The fractional uncertainty ( $f$ ) is provided in Table D1.

**Table D1. Fractional uncertainty for PM<sub>2.5</sub> and PM<sub>10</sub> applied within specific date ranges.**

Species	f (2/28/1995 – 12/31/2006)	f (1/1/2017 – 12/31/2017)	f (1/1/2018 – 12/31/2018)	f (1/1/2019 – 12/31/2019)	f (1/1/2020 – current)
PM <sub>2.5</sub>	0.03	0.03	0.04	0.04	0.04
PM <sub>10</sub>	0.03	0.07	0.07	0.08	0.07

### *Ions (B Module)*

Ions are measured by ion chromatography using the nylon filter from the B module. Ion data are reported in  $\mu\text{g filter}^{-1}$  before conversion to concentration. The concentration ( $C_{\text{ion}}$ ), uncertainty ( $\sigma_{\text{ion}}$ ), and MDL ( $\text{mdl}_{\text{ion}}$ ) are calculated for the ion species using the following equations; however, for nitrite, when the concentration is less than or equal to zero, uncertainty is reported as zero. Units are  $\mu\text{g m}^{-3}$

$$C_{ion} = \frac{(A_{ion} - B_{ion})}{V_{B\ module}} \quad (D4)$$

$$\sigma_{ion} = \frac{\sqrt{(0.608 \times \text{Max}(P95 - B_{ion}, \text{mdl}_{\text{analytical}}))^2 + (f \times (A_{ion} - B_{ion}))^2}}{V_{B\ Module}} \quad (D5)$$

$$\text{mdl}_{ion} = \frac{\text{Max}(P95 - B_{ion}, \text{mdl}_{\text{analytical}})}{V_{B\ Module}} \quad (D6)$$

The ambient mass loading is  $A_{ion}$  ( $\mu\text{g filter}^{-1}$ ).  $B_{ion}$  is the median of the field blank mass loading in  $\mu\text{g filter}^{-1}$  when there are  $\geq 50$  field blanks in a month; otherwise, values from the previous month are used. The B-module sample air volume ( $\text{m}^3$ ) is  $V_{B\ module}$ . P95 is the 95<sup>th</sup> percentile of field blank measurements in  $\mu\text{g filter}^{-1}$ . The analytical MDL ( $\text{mdl}_{\text{analytical}}$ ) in  $\mu\text{g filter}^{-1}$  is reported from the analytical laboratory (Table D2). The analytical MDL is considered the ‘floor value’ and is used as the reported MDL in the event that the median value of the field blanks is lower than the respective analytical MDL. The value of 0.608 (=1/1.645) is used to estimate the one-sigma uncertainty at zero concentration from the MDL that is set at the 95th percentile, where 1.645 is the critical value for sigma in a one-tailed test for 5% significance. The fractional uncertainty (f) is given in Table D3.

**Table D2. Analytical method minimum detection limits (MDL) in  $\mu\text{g filter}^{-1}$  applied within specific date ranges.**

Species	Analytical MDLs (1/1/2006 – 12/31/2019)	Analytical MDLs (1/1/2020 – current)
Chloride ( $\text{Cl}^-$ )	0.03	0.1
Nitrite ( $\text{NO}_2^-$ )	0.01	0.2
Nitrate ( $\text{NO}_3^-$ )	0.05	0.16
Sulfate ( $\text{SO}_4^{2-}$ )	0.07	0.22

**Table D3. Fractional uncertainty (f) for ions applied within specific date ranges.**

Species	f (1/1/2005 – 12/31/2016)	f (1/1/2017 – 12/31/2017)	f (1/1/2018 – 12/31/2018)	f (1/1/2019 – 12/31/2019)	f (1/1/2020 – current)
Chloride ( $\text{Cl}^-$ )	0.08	0.08	0.08	0.09	0.10
Nitrite ( $\text{NO}_2^-$ )	0.22	0.25	0.25	0.25	0.25
Nitrate ( $\text{NO}_3^-$ )	0.04	0.03	0.04	0.04	0.04
Sulfate ( $\text{SO}_4^{2-}$ )	0.02	0.02	0.02	0.03	0.02

*Carbon (C Module)*

Carbon is measured by thermal optical reflectance (TOR) and thermal optical transmittance (TOT) using the quartz filter from the C Module. The seven carbon fractions (OC1-OC4, EC1-EC3) and organic pyrolyzed carbon (OP) are recorded in  $\mu\text{g filter}^{-1}$ . For the carbon fractions, the primary factors that determine the fractional uncertainty are the homogeneity of the sample deposit and the accuracy of the temperature set point in each stage. For OP, the primary factors that determine the fractional uncertainty are the laser signal stability and the accuracy of the split point placement.

The concentration (C), uncertainty ( $\sigma_{\text{Carbon}}$ ), and MDL ( $\text{mdl}_{\text{Carbon}}$ ) in  $\mu\text{g m}^{-3}$  for the carbon species (OC1, OC2, OC3, OC4, OP, OP, EC1, EC2, and EC3) are calculated using the following equations:

$$C = \frac{A_{\text{Carbon}} - B_{\text{Carbon}}}{V_{\text{C Module}}} \quad (\text{D7})$$

$$\sigma_{\text{Carbon}} = \frac{\sqrt{(0.608 \times \text{Max}(P95 - B_{\text{Carbon}}, \text{mdl}_{\text{analytical}}))^2 + (f \times (A_{\text{Carbon}} - B_{\text{Carbon}}))^2}}{V_{\text{C Module}}} \quad (\text{D8})$$

$$\text{mdl}_{\text{Carbon}} = \frac{\text{Max}(P95 - B_{\text{Carbon}}, \text{mdl}_{\text{analytical}})}{V_{\text{C Module}}} \quad (\text{D9})$$

The ambient mass loading ( $A_{\text{Carbon}}$ ) is in units of  $\mu\text{g filter}^{-1}$ . The median of the field blank mass loading is  $B_{\text{Carbon}}$  ( $\mu\text{g filter}^{-1}$ ) when there are  $\geq 50$  field blanks in that month, otherwise the number from the previous month is used.  $V_{\text{C Module}}$  is the C module sample air volume ( $\text{m}^3$ ) and P95 is the 95<sup>th</sup> percentile of field blank measurements ( $\mu\text{g filter}^{-1}$ ). The analytical MDL ( $\text{mdl}_{\text{analytical}}$ ,  $\mu\text{g filter}^{-1}$ ) is reported from the analytical laboratory (Table D4). The analytical MDL is considered the ‘floor value’ and is used as the reported MDL in the event that the median value of the field blanks is lower than the respective analytical MDL. The value of 0.608 ( $=1/1.645$ ) is used to estimate the one-sigma uncertainty at zero concentration from the MDL that is set at the 95th percentile, where 1.645 is the critical value for sigma in a one-tailed test for 5% significance. The fractional uncertainty (f) is given in Table D5.

**Table D4. Analytical method minimum detection limits (MDL) in  $\mu\text{g filter}^{-1}$  for carbon species applied within specific date ranges. “R” refers to reflectance and “T” refers to transmittance. TC is total carbon (OC+EC) from reflectance.**

Species	Analytical MDL (1/1/2006 – 12/31/2019)	Analytical MDL (1/1/2020 – current)
OC1	0.51	0.03
OC2	0.51	0.06
OC3	0.51	0.18
OC4	0.51	0.12
OPTR	0.15	0.12
OPTR at 405 nm	0.15	0.03

Species	Analytical MDL (1/1/2006 – 12/31/2019)	Analytical MDL (1/1/2020 – current)
OPTR at 445 nm	0.15	0.06
OPTR at 532 nm	0.15	0.08
OPTR at 780 nm	0.15	0.08
OPTR at 808 nm	0.15	0.06
OPTR at 980 nm	0.15	0.12
OPTT	0.15	0.22
OPTT at 405 nm	0.15	0.18
OPTT at 445 nm	0.15	0.21
OPTT at 532 nm	0.15	0.19
OPTT at 780 nm	0.15	0.2
OPTT at 808 nm	0.15	0.19
OPTT at 980 nm	0.15	0.15
EC1	0.15	0.07
EC2	0.15	0.22
EC3	0.15	0.01
ECTR	0.15	0.23
OCTR	0.51	0.31
TC	0.57	0.43

**Table D5. Fractional uncertainty (f) for carbon species applied within specific date ranges. Prior to 2017, data for OP at different wavelengths were not reported.**

Species	f (1/1/2005 – 12/31/2016)	f (1/1/2017 – 12/31/2017)	f (1/1/2018 – 12/31/2018)	f (1/1/2019 – 12/31/2019)	f (1/1/2020 – current)
OC1	0.23	0.27	0.23	0.24	0.21
OC2	0.15	0.13	0.11	0.10	0.09
OC3	0.13	0.13	0.13	0.11	0.09
OC4	0.15	0.13	0.13	0.14	0.16
OPTR	0.13	0.16	0.20	0.21	0.20
OPTR at 405 nm	N/A	0.18	0.18	0.19	0.19

Species	f (1/1/2005 – 12/31/2016)	f (1/1/2017 – 12/31/2017)	f (1/1/2018 – 12/31/2018)	f (1/1/2019 – 12/31/2019)	f (1/1/2020 – current)
OPTR at 445 nm	N/A	0.17	0.17	0.18	0.18
OPTR at 532 nm	N/A	0.20	0.21	0.21	0.21
OPTR at 780 nm	N/A	0.19	0.21	0.22	0.22
OPTR at 808 nm	N/A	0.19	0.20	0.21	0.22
OPTR at 980 nm	N/A	0.21	0.23	0.25	0.25
OPTT	0.13	0.12	0.14	0.15	0.14
OPTT at 405 nm	N/A	0.13	0.13	0.14	0.13
OPTT at 445 nm	N/A	0.13	0.13	0.15	0.14
OPTT at 532 nm	N/A	0.13	0.14	0.15	0.14
OPTT at 780 nm	N/A	0.13	0.14	0.16	0.14
OPTT at 808 nm	N/A	0.13	0.15	0.16	0.15
OPTT at 980 nm	N/A	0.14	0.16	0.17	0.15
EC1	0.10	0.10	0.11	0.11	0.11
EC2	0.17	0.18	0.19	0.21	0.22
EC3	0.42	0.25	0.25	0.25	0.25
ECTR	0.12	0.14	0.14	0.13	0.13
OCTR	0.08	0.09	0.08	0.07	0.07
TC	0.08	0.08	0.07	0.07	0.06

### Elements (A Module)

Elements are measured using X-ray fluorescence (XRF; PANalytical Epsilon 5) using the Teflon filters from the A module. The PANalytical XRF instruments report the elements in terms of counts per mV per second, which is converted into areal densities using element calibration. Blank subtraction is performed on the XRF measurements by subtracting the median field blank count from the same filter lot as that of the sample filters. The field blank correction is specific to each filter lot and since the number of field blanks from a filter lot used in a given month may not be statistically sufficient, a minimum of 35 field blanks are required before the median can be calculated. Field blank selection is therefore expanded to include field blanks from previous month(s) until at least 35 field blanks are found. The selected 35 field blanks are

used to calculate batch and filter lot specific blank correction. Areal density ( $A_e$ ), areal uncertainty ( $U_{element}$ ), and areal analytical MDL ( $mdl_{analytical}$ ,  $\mu\text{g cm}^{-2}$ ) are calculated during processing of XRF results.  $U_{element}$  is calculated as:

$$U_{element} = \sqrt{\left(0.608 \times \text{Max}\left((P95 - B_e), mdl_{analytical}\right)\right)^2 + \left(f \times (A_e - B_e)\right)^2} \quad (\text{D10})$$

The median areal density ( $B_e$ ) of the field blank is measured by XRF with  $\geq 35$  field blanks from before the determination date. P95 is the 95<sup>th</sup> percentile of field blank measured by XRF. The  $mdl_{analytical}$  is reported from the analytical laboratory (Table D6). The  $mdl_{analytical}$  is considered the ‘floor value’ and is used as the reported MDL in the event that the median value of the field blanks is lower than the respective analytical MDL. The fractional uncertainty ( $f$ ) is given in Table D7. The value of 0.608 (=1/1.645) is used to estimate the one-sigma uncertainty at zero concentration from the MDL that is set at the 95th percentile, where 1.645 is the critical value for sigma in a one-tailed test for 5% significance.

The concentration ( $C_{element}$ ), uncertainty ( $\sigma_{element}$ ), and MDL ( $mdl_{element}$ ) in  $\mu\text{g m}^{-3}$  for the element species are calculated using the following equations:

$$C_{element} = \frac{(A_e - B_e) \times (\text{Deposit area})}{V} \quad (\text{D11})$$

$$\sigma_{element} = \frac{(U_{element}) \times (\text{Deposit area})}{V} \quad (\text{D12})$$

$$mdl_{element} = \frac{\text{Max}\left((P95 - B_e), mdl_{analytical}\right) \times (\text{Deposit area})}{V} \quad (\text{D13})$$

The deposit area is the area of deposit on the filter ( $\text{cm}^2$ ), determined from the filter holder or mask size ( $3.53 \text{ cm}^2$ ) and  $V$  is the sample air volume ( $\text{m}^3$ ).

**Table D6. Analytical method minimum detection limit (MDL) in  $\mu\text{g cm}^{-2}$  for elemental species applied within specific date ranges.**

Species	Analytical MDL (1/1/2006 – 12/31/2019)	Analytical MDL (1/1/2020 – current)
Al	0.011	0.011
As	0.002	0.002
Br	0.001	0.001
Ca	0.021	0.003
Cl	0.002	0.002
Cr	0.001	0.001

Species	Analytical MDL (1/1/2006 – 12/31/2019)	Analytical MDL (1/1/2020 – current)
Cu	0.002	0.001
Fe	0.012	0.003
K	0.005	0.001
Mg	0.021	0.02
Mn	0.003	0.002
Na	0.037	0.046
Ni	0.001	0.001
P	0.002	0.002
Pb	0.006	0.003
Rb	0.002	0.002
S	0.003	0.001
Se	0.002	0.001
Si	0.013	0.005
Sr	0.002	0.001
Ti	0.003	0.001
V	0.001	0.001
Zn	0.002	0.002
Zr	0.012	0.007

**Table D7. Fractional uncertainty (f) for elemental species applied within specific date ranges.**

Species	f (1/1/2005 – 12/31/2016)	f (1/1/2017 – 12/31/2017)	f (1/1/2018 – 12/31/2018)	f (1/1/2019 – 12/31/2019)	f (1/1/2020 - current)
Al	0.09	0.08	0.08	0.09	0.10
As	0.25	0.21	0.25	0.25	0.25
Br	0.10	0.11	0.10	0.09	0.09

Species	f (1/1/2005 – 12/31/2016)	f (1/1/2017 – 12/31/2017)	f (1/1/2018 – 12/31/2018)	f (1/1/2019 – 12/31/2019)	f (1/1/2020 - current)
Ca	0.06	0.07	0.06	0.07	0.09
Cl	0.14	0.18	0.14	0.14	0.16
Cr	0.22	0.17	0.15	0.17	0.16
Cu	0.12	0.11	0.13	0.10	0.10
Fe	0.06	0.06	0.05	0.06	0.08
K	0.03	0.05	0.03	0.04	0.05
Mg	0.15	0.16	0.15	0.15	0.17
Mn	0.13	0.13	0.14	0.13	0.13
Na	0.14	0.15	0.14	0.14	0.15
Ni	0.16	0.16	0.13	0.14	0.18
P	0.25	0.33	0.27	0.30	0.30
Pb	0.13	0.13	0.14	0.15	0.25
Rb	0.25	0.25	0.25	0.25	0.25
S	0.03	0.03	0.02	0.03	0.03
Se	0.25	0.12	0.25	0.25	0.25
Si	0.10	0.07	0.06	0.07	0.09
Sr	0.16	0.14	0.13	0.14	0.14
Ti	0.11	0.09	0.09	0.09	0.11
V	0.12	0.14	0.17	0.17	0.12
Zn	0.06	0.08	0.08	0.08	0.08
Zr	0.25	0.25	0.25	0.25	0.25

### *Filter Absorption (A Module)*

Optical absorption is measured by a hybrid integrating plate and sphere (HIPS) system using the Teflon filter from the A module. The laser absorption measurements are reflectance (R) and

transmittance (T) values. Results from the HIPS measurement are reported as filter absorption coefficient (fabs) in units of  $\text{Mm}^{-1}$ , calculated from R and T. The coefficient is calculated with equation D14:

$$f_{abs} = 100 \times \frac{\tau_{633} \times (\text{Deposit area})}{V_{A-\text{module}}} \quad (\text{D14})$$

where the volume ( $V_{A-\text{Module}}$ ) is the A module sample air volume ( $\text{m}^3$ ), the deposit area is the area of sample deposit on the filter ( $3.53 \text{ cm}^2$ ), determined from the filter holder or mask size, and the optical depth ( $\tau_{633}$ ), is calculated with equation D15. The slope and intercept are derived from a linear regression field blanks to transform the raw T and R values to the field blank corrected values. More information on derivation of  $f_{abs}$  is available in the [SOP](#).

$$\tau_{633} = \log \left( \text{Max} \left( \frac{\text{intercept} + (\text{slope} \times R)}{T}, 0.1 \right) \right) \quad (\text{D15})$$

The uncertainty ( $\sigma_{fabs}$ ) is given as:

$$\sigma_{fabs} = 100 \times \frac{\sqrt{\left( 0.608 \times \text{Max}(P95, \text{mdl}_{\text{analytical}}) \right)^2 + (f_{\text{unitless}} \times \tau_{633})^2 \times (\text{Deposit area})}}{V_{A-\text{module}}} \quad (\text{D16})$$

P95 is the 95<sup>th</sup> percentile of field blank measurements and the analytical MDL( $\text{mdl}_{\text{analytical}}$ ) is reported from the analytical laboratory ( $\tau_{633} = 0.009$ , unitless). The  $\text{mdl}_{\text{analytical}}$  is considered the 'floor value' and is used as the reported MDL in the event that the median value of the field blanks is lower than the respective analytical MDL. The A module air volume ( $\text{m}^3$ ) is given by  $V_{A-\text{Module}}$  and the deposit area is the area of sample deposit on the filter ( $3.53 \text{ cm}^2$ ). The unitless fractional uncertainty ( $f_{\text{unitless}}$ ) is calculated from fractional uncertainty (Table D8) and nominal sample volume. The value of 0.608 (=1/1.645) is used to estimate the one-sigma uncertainty at zero concentration from the MDL that is set at the 95th percentile, where 1.645 is the critical value for sigma in a one-tailed test for 5% significance. The MDL for fabs ( $\text{mdl}_{\text{fabs}}$ ) is given by equation D17:

$$\text{mdl}_{\text{fabs}} = 100 \times \frac{\text{Max}(P95, \text{mdl}_{\text{analytical}}) \times (\text{Deposit area})}{V_{A-\text{module}}} \quad (\text{D17})$$

**Table D8. Fractional uncertainty (f) for filter absorption data applied within specific date ranges.**

Species	f (2/28/1995 – 12/31/2006)	f (1/1/2017 – 12/31/2017)	f (1/1/2018 – 12/31/2018)	f (1/1/2019 – 12/31/2019)	f (1/1/2020 – current)
fabs	0.03	0.06	0.06	0.05	0.06